THE HYGROSCOPICITY PARAMETER
OF MARINE ORGANICS IN SEA SPRAY
AEROSOLS

by

Matthew Boyer

Submitted in partial fulfilment of the requirements
for the degree of Master of Science

at

Dalhousie University
Halifax, Nova Scotia
January 2017

TABLE OF CONTENTS

LIST OF TABLES

LIST OF FIGURES

ABSTRACT

Atmospheric aerosols have important implications on Earth's radiation budget by scattering and absorbing incoming solar radiation either directly or indirectly through cloud processes. Aerosols have a net cooling effect on climate, which opposes the warming caused by greenhouse gases. The magnitude of cooling, however, is poorly constrained due to large uncertainties associated with natural aerosol sources and their interactions with clouds. As oceans cover 70% of the earth's surface, sea spray aerosols (SSA), which act efficiently as cloud condensation nuclei (CCN), are an important source of natural aerosol emissions. Surface active organic compounds readily accumulate in the sea surface microlayer (SML) and transfer onto SSA during bubble bursting; however, the resulting effects of organic content on CCN activation remains unresolved. Consequently, the work in this thesis proposes and tests a desalting method for quantifying the cloud nucleating properties of the organic components in surface seawater using κ-Köhler theory.

CCN measurements were used to infer the hygroscopicity parameter (κ) of atomized particles generated from ambient SML and bulk seawater samples. Using analyses of seawater chemistry, the concentration of organic and inorganic components in the particles were quantified. Even after desalting, inorganic constituents dominate the particle composition (>97%). Comparisons of hygroscopicity measurements in the samples before and after desalting show a significant reduction in κ (47 – 62%), which is inconsistent with κ-Köhler theory predictions. The project is still a work in progress; additional experiments are necessary to provide conclusive results on the mechanism contributing to the discrepancy between the observations and theoretical predictions.

LIST OF ABBREVIATIONS AND SYMBOLS USED

a_w	Activity of water
f_{ccn}	Fraction of activated cloud condensation nuclei
ε	Volume fraction
ε_{inorg}	Volume fraction of inorganic component
ε_{org}	Volume fraction of organic component
κ	Hygroscopicity parameter
κ_{inf}	Hygroscopicity parameter inferred from measurements
κ_{inorg}	Hygroscopicity parameter for inorganic component
κ_{org}	Hygroscopicity parameter for organic component
κ_{tot}	Hygroscopicity parameter for an entire particle
n_s	Moles of solute
n_w	Moles of water
ρ_w	Density of water
ρ_{inorg}	Density of inorganic components
ρ_{org}	Density of organic components
σ	Standard Deviation
$\sigma_{s/a}$	Surface tension at the interface of a solution
i	Van't Hoff factor
μm	Micrometer
μL	Microliter
$°C$	Degrees Centigrade
ACSM	Aerosol Chemical Speciation Monitor
BSA	Bovine serum albumin
Ca^{2+}	Dissolved calcium ion
CCN	Cloud condensation nuclei
Cl^-	Dissolved chloride ion
cm	Centimeter

CO_2	Carbon Dioxide
CPC	Condensation Particle Counter
D	Wet droplet diameter
Da	Dalton
D_c	Critical dry particle diameter
D_d	Dry particle diameter
DMA	Differential Mobility Analyzer
DOM	Dissolved organic matter
DOC	Dissolved organic carbon
F^-	Dissolved fluoride ion
g	Gram
GPS	Global Positioning System
HCl	Hydrochloric acid
IC	Ion chromatography
IPCC	Intergovernmental Panel on Climate Change
J	Joule
K	Kelvin
kg	Kilogram
L	Liter
m	Meter
M	Molarity
mf_{inorg}	Mass fraction of inorganic components
mf_{org}	Mass fraction of organic components
mM	Millimolar
mg	Milligram
Mg^{2+}	Dissolved Magnesium ion
mL	Milliliter
mm	Millimeter
mol	Mole
M_w	Molecular weight
MWCO	Molecular weight cut off
Na^+	Dissolved sodium ion

NaCl	Sodium chloride
NIR	Near infrared spectrum
nm	Nanometer
OM/OC	Ratio of organic matter to organic carbon
ppb	Parts per billion
ppm	Parts per million
ppt	Parts per thousand
PTFE	Polytetrafluoroethylene (Teflon)
R	Universal Gas Constant
s	Saturation ration
S	Supersaturation
S_c	Critical supersaturation
SSA	Sea spray aerosol
SML	Sea surface microlayer
SO_4^{2-}	Dissolved sulfate ion
SW	Seawater
T	Temperature
UV	Ultra violet spectrum
Vf_{org}	Volume fraction of organic components
Vis	Visible spectrum
Yr	Year

ACKNOWLEDGEMENTS

CHAPTER 1   INTRODUCTION

1.1 Aerosols in the Atmosphere

Aerosols, or small solid and liquid particles suspended in the atmosphere, are ubiquitous and have important implications on human health and climate. Large sources of aerosol emissions exist from both natural and anthropogenic sources; Fossil fuel combustion, industry, and transportation comprise the major contributions from anthropogenic sources, whereas mineral dust, boreal biomass burning, volcanoes, and sea spray aerosols are the primary sources of natural aerosols emissions. The size of the particles in the atmosphere spans several orders of magnitude: from tens of angstroms to hundreds of micrometers in diameter. In typical ambient aerosol, the particle size distribution can be divided into four distinct modes: the nucleation mode (< 10 nm), the Aitken mode (10 – 100 nm), the accumulation mode (100 nm – 2.5 µm), and the coarse mode (> 2.5 µm). Particles in each mode have distinct characteristics in terms of sources, composition, and behavior in the atmosphere, including removal processes, climate effects, and human health impacts (Seinfeld and Pandis, 2006).

The smallest sized particles, the nucleation mode, are formed from precursor gases in the atmosphere that can nucleate and form new particles. Additional gases can continue to condense onto the nucleated particles, which allows them to grow into the Aitken mode size range. The nucleation and Aitken mode particles dominate in total atmospheric aerosol number concentrations; however, their influence in total aerosol mass is very small, comprising only a few percent (Fitzgerald, 1991). Coagulation with larger particles

accounts for the loss of most of the particles in the two smallest modes. The particles in the Aitken mode that are not lost to coagulation can grow further by condensation into the accumulation mode. The accumulation mode particles, which are less prone to loss through coagulation and dry deposition, have the longest atmospheric lifetimes and contribute significantly to total atmospheric aerosol mass and surface area. In the coarse mode, particles are often primary in origin; they are typically sourced from mechanical processes and include mineral dust and sea spray aerosol. The larger size of the coarse mode particles makes them more subject to dry deposition processes, leading to shorter residence times in the atmosphere (Seinfeld and Pandis, 2006).

1.2 Climate Effects of Aerosols

Aerosols have important impacts on Earth's climate by influencing the radiative properties of the atmosphere. The current understanding implies that aerosols in the atmosphere have an influence on radiative forcing that opposes the warming effect of greenhouse gases; however, the extent that aerosols can contribute to surface cooling is largely uncertain and poorly represented by modern climate models (IPCC, 2013). Additionally, the concentration of aerosols in the atmosphere has been increasing since the industrial revolution as a result of an increase in anthropogenic aerosol production. Higher aerosol concentrations suggest that the climate effects of aerosols have become more prominent over time as well (Seinfeld and Pandis, 2006). Two major effects of aerosols on climate have been identified: the direct and indirect radiative effects. While the direct effect is important for modeling the total radiative forcing due to atmospheric aerosol, the research

presented in this thesis focuses primarily on the aerosol indirect effects. Therefore, in the following discussion, the indirect effect of aerosols is presented in greater detail.

1.2.1   The Direct Effect

The direct effect is characterized by the scatter and absorption of incoming solar radiation by atmospheric particles, a process which can contribute to surface cooling by preventing the radiation from reaching Earth's surface. The aerosol size distribution, number concentration, and composition controls the efficiency of scatter and absorption of incoming solar radiation by the aerosol direct effect. Furthermore, particles with a diameter smaller than 1 μm are the most effective at scattering incoming solar radiation (Seinfeld and Pandis, 2006).

1.2.2   The Indirect Effect

Aerosols can interact with and influence the radiative properties and behavior of clouds in the atmosphere. The absorption and reflection properties of the resulting clouds, which can also contribute to climate forcing, comprises the aerosol indirect effect. The presence of a high energy barrier prevents the direct condensation of water vapor through homogenous processes in the atmosphere. As a result, cloud droplet formation is a heterogeneous process, requiring the presence of a particle to act as a substrate upon which water vapor can condense (Pruppacher and Klett, 1997). The particles that are able to serve as a substrate for cloud droplets are referred to as cloud condensation nuclei (CCN). The cloud droplet number in a cloud has direct implications on the properties of the cloud. Therefore,

changes induced by the addition of particles that can activate as CCN in a cloud can alter the radiation budget at the earth's surface.

Previous research has identified two major aerosol-cloud interactions induced by increases in aerosol concentrations in the atmosphere that are relevant for climate: the cloud albedo effect (Twomey, 1997) and the cloud lifetime effect (Albrecht, 1989). Both of these effects result from changes in cloud droplet sizes under conditions where higher concentrations of CCN are present in a cloud, as summarized in Figure 1.1.

A study conducted by Twomey (1977) shows that clouds that form downwind of polluted regions are more efficient at reflecting incoming short wave radiation. This effect, caused by an increase in particle number that yields a higher concentration of CCN in the clouds, is the cloud albedo effect (Twomey, 1977). A similar increase in cloud reflectivity has also been observed in clouds influenced by ship track emissions in the marine boundary layer, providing additional evidence of the cloud albedo effect (Coakley et al., 1987).
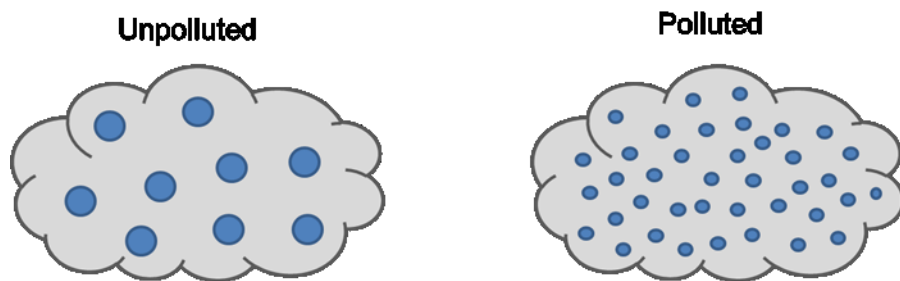
Figure 1.1   Diagram illustrating the differences in cloud droplet size between clouds for clean and polluted regimes. When the liquid water content of the cloud remains constant, the presence of more CCN in the cloud causes the cloud droplets to be smaller in size because their growth is limited by the available water vapor. Smaller cloud droplets lead to higher reflectivity (the cloud albedo effect) and prolong the cloud's atmospheric lifetime (the cloud lifetime effect).

Furthermore, under clean conditions (e.g. remote locations in the marine boundary layer), even modest increases in CCN have been identified to have significant implications on the albedo of clouds (Murphy et al., 1998).

In addition to the cloud albedo effect, smaller droplets in a cloud also give rise to the cloud lifetime effect. Under cleaner conditions with the presence of less particles, cloud droplets are able to grow larger and favorably fall as precipitation. Assuming the liquid water content of a cloud remains the same, the introduction of more CCN limits the growth of droplets in the cloud because the CCN 'compete' for available water vapor (Lohmann and Feichter, 2005). As a result, precipitation from the cloud is suppressed, which increases the atmospheric lifetime of the cloud (Albrecht, 1989). Therefore, the effects of additional CCN in a cloud are twofold on climate: the clouds that form are more reflective and persist for longer durations in the atmosphere.

The Intergovernmental Panel on Climate Change (IPCC) classifies the aerosol indirect effect as the most significant source of uncertainty in the current understanding of climate forcing (Figure 1.2) (IPCC, 2013). The current level of confidence associated with the science surrounding the indirect effect is low, indicating that many questions remain unanswered (Boucher et al., 2013). A significant portion of this uncertainty stems from the current lack of understanding of natural aerosol in the background and their effect on cloud properties (Carslaw et al., 2013), as well as the poor characterization of organics that can act as CCN (IPCC, 2013). As such, knowledge of the cloud nucleating properties of aerosols in the atmosphere is of particular importance to understanding the effect that clouds have on climate and improving climate projection models.

Emitted compound	Resulting atmospheric drivers	Radiative forcing by emissions and drivers	Level of confidence
CO_2	CO_2	1.68 [1.33 to 2.03]	VH
CH_4	CO_2 H_2O^{str} O_3 CH_4	0.97 [0.74 to 1.20]	H
Halo-carbons	O_3 CFCs HCFCs	0.18 [0.01 to 0.35]	H
N_2O	N_2O	0.17 [0.13 to 0.21]	VH
CO	CO_2 CH_4 O_3	0.23 [0.16 to 0.30]	M
NMVOC	CO_2 CH_4 O_3	0.10 [0.05 to 0.15]	M
NO_x	Nitrate CH_4 O_3	-0.15 [-0.34 to 0.03]	M
Aerosols and precursors (Mineral dust, SO_x, NH_3, Organic carbon and Black carbon)	Mineral dust Sulphate Nitrate Organic carbon Black carbon	-0.27 [-0.77 to 0.23]	H
	Cloud adjustments due to aerosols	-0.55 [-1.33 to -0.06]	L
Albedo change due to land use		-0.15 [-0.25 to -0.05]	M
Changes in solar irradiance		0.05 [0.00 to 0.10]	M
Total anthropogenic RF relative to 1750	2011	2.29 [1.13 to 3.33]	H
	1980	1.25 [0.64 to 1.86]	H
	1950	0.57 [0.29 to 0.85]	M

Radiative forcing relative to 1750 (W m⁻²)

Figure 1.2   A summary of atmospheric radiative forcing since the industrial revolution due to natural and anthropogenic process. The research evidence suggests that the indirect aerosol effects are important for offsetting the radiative forcing associated with greenhouse gas emissions, yet the magnitude of such effects are poorly constrained and constitute the greatest uncertainty in climate forcing. Adapted from (IPCC, 2013).

1.3 κ-Köhler Theory

The ability to predict CCN activation in aerosols is crucial given the large uncertainty associated with the indirect effect. Previous research has aimed to characterize and predict cloud droplet formation in atmospheric aerosol. The most influential work, known as Köhler theory, created a foundation for the development of an additional parameterization, called κ-Köhler theory. These parameterizations are widely used in current cloud

microphysical research and are fundamental to the research question outlined in this thesis. Therefore, a background of their principles and application are presented below.

In 1936, Hilding Köhler published ground-breaking research for cloud microphysics. His work provides a framework to predict the cloud droplet activity of a particle based on two thermodynamic principles that influence water vapor equilibrium in an activating droplet: the Kelvin effect and Raoult's law. The Kelvin effect describes the role that a curved droplet surface and surface tension have on the water vapor equilibrium, and Raoult's law defines the solute effects based on the particle composition. These two terms combined into a single equation are called the Köhler equation, or Köhler theory (Köhler, 1936). Using Köhler theory, the saturation ratio at which an aerosol of known composition will activate can be predicted. In the atmosphere, supersaturations in clouds generally range between 0.05 - 0.8 % (Pruppacher and Klett, 1997). The saturation ratio (s), or the water vapor pressure above an activating droplet, is often expressed as supersaturation (S), or the saturation of water vapor over 100%, as per the following relationship:

$$s = \frac{S}{100\%} + 1 \tag{1.1}$$

Köhler theory is defined by the following equation (Pruppacher and Klett, 1997):

$$s = a_w \exp\left(\frac{4\sigma_{s/a} M_w}{RT \rho_w D}\right) \tag{1.2}$$

where a_w is the activity of water, $\sigma_{s/a}$ is the surface tension at the interface of the solution, M_w is the molecular weight of water, R is the universal gas constant (8.314 J mol^{-1} K^{-1}), T is the temperature, ρ_w is the density of water, and D is the wet diameter of the droplet. The activity of water can be defined as (Kreidenweis et al., 2005):

$$a_w^{-1} = 1 + i \frac{n_s}{n_w} \tag{1.3}$$

where i is the Van't Hoff factor, n_s is moles of solute, and n_w is moles of water. The Van't Hoff factor is the number of discrete ions in a solution that result from the dissolution of a given compound (i.e. NaCl dissociates to Na$^+$ and Cl$^-$, $i = 2$). Despite additional modifications to the original Köhler equation over time (McDonald, 1953; Low 1969), the version of Köhler theory using the Van't Hoff factor (equations 1.2 & 1.3) was shown to yield predictions that are the most representative of experimental data (Chylek and Wong, 1998), and is the most commonly used expression of Köhler theory (Pruppacher and Klett, 1997; Kreidenweis et al., 2005). Previous laboratory studies have utilized Köhler theory to predict droplet activation, including organic (Kumar et al., 2003; Broekhuizen et al., 2004) and mixed component aerosol (Prisle et al., 2010).

As is apparent from equation 1.3, the application of Köhler theory to predict cloud droplet formation requires specific knowledge of aerosol composition and properties, including mass, molecular weight, density, number of dissociable ions, and activity coefficients (Petters and Kreidenweis, 2007). When performing analyses on ambient aerosol, such properties are unknown, which forbids a quantitative prediction for CCN activation. Aerosol composition in the atmosphere is complex; composition measurements of ambient

aerosol show that the majority of particles exist in mixed states containing both inorganic and organic components (Pratt and Prather, 2010), and estimates of the number of different organic compounds present in such particles range between 10,000 -100,000 (Goldstein and Galbally, 2007). Therefore, the use of Köhler theory is not feasible on ambient aerosol.

To resolve the issue of unknown composition, Petters and Kreidenweis (2007) developed a parameterized version of Köhler theory, called κ-Köhler theory. The parameterization simplifies the water activity term using a hygroscopicity parameter, κ. κ-Köhler theory is defined by the following equation:

$$S(D) = \frac{D^3 - D_d{}^3}{D^3 - D_d{}^3(1-k)} \exp\left(\frac{4\sigma M_w}{RT\rho_w D}\right) \tag{1.4}$$

where D_d is the dry particle diameter, and κ is the hygroscopicity parameter. Expressing equation 1.4 in terms of κ yields:

$$k = \frac{4A^3}{27D_d{}^3 \ln^2 S_c} \tag{1.5}$$

where:

$$A = \frac{4\sigma M_w}{RT\rho_w} \tag{1.6}$$

Using equation 1.5 and 1.6, the hygroscopicity parameter can be calculated experimentally, which allows it to be applied to ambient aerosol or particles of unknown composition. The terms in equation 1.6 are either constant or properties of water that remain constant ($\sigma = 0.072$ J m^{-2}, $M_w = 18.02$ g mol^{-1}, $R = 8.314$ J mol^{-1} K^{-1}, $T = 298$ K,

$\rho_w = 1000$ kg m^{-3}); thus, A is constant. As a result, the supersaturation (S$_c$) and dry particle diameter (D$_d$) are the only variables in equation 1.5. In this case, S$_c$ is defined as the critical supersaturation, or the supersaturation at which the particles activate into cloud droplets. When making CCN activation measurements, S$_c$ and D$_d$ are variables that are controlled via instrumentation (See Section 3.3.5 and 3.3.3). Therefore, using CCN measurements, κ can be calculated. The specific procedure for inferring κ from measurements at supersaturated conditions is discussed in detail in Section 3.4. κ can also be inferred from hygroscopic growth measurements in sub-saturated conditions, however, this method is not discussed, as it is not used in the experiments contained in this thesis.

Table 2.1   Typical ranges of κ in aerosol. Organic compounds, which are less hygroscopic, typically have lower κ values (Petters and Kreidenweiss, 2007).

Species	κ Range
Organics	0.01 - 0.5
Inorganic Salts	0.5 - 1.4
Atmospheric Aerosol	$0.1 < \kappa < 0.9$

κ-Köhler theory also provides a framework for handling mixed-component particles. In an internally mixed particle, κ can be further broken down by the hygroscopicity of the different components. Table 1.1 summarizes the typical ranges of κ observed for organics, inorganics, and atmospheric aerosol. When the volume fraction (ε) and κ of each component i in the particle is known, the overall κ of the particle (κ_{tot}) is given by the following relationship:

$$K_{tot} = \sum \varepsilon_i k_i \qquad (1.7)$$

In addition to its application for unknown aerosol and internally mixed compositions, the simplicity of using a single hygroscopicity parameter to characterize the CCN activity of different types of aerosol also allows for easy incorporation into climate models without large computational costs (Petters and Kreidenweiss, 2007).

CHAPTER 2   SEA SPRAY AEROSOLS

In this chapter, the topic of aerosols and their impact in the atmosphere is narrowed to a

discussion of sea spray aerosols (SSA) and their importance in the marine boundary layer.

The discussion begins by explaining SSA production by bubble busting, and then relates

this process to SSA fluxes, size distributions, composition, and climate effects.

Additionally, the concept of the sea surface microlayer is presented, specifically

highlighting its role in SSA formation and composition. The chapter also provides a brief

review of the scientific literature on SSA, with a focus on the prevalence of the organic

composition in SSA to motivate its importance on the effects that marine organics have on

CCN activity. Lastly, the chapter summarizes the principle objectives of the research

presented in this thesis.

2.1 SSA Production

Due to the large percentage of ocean coverage on Earth (~70%), SSA, or primary aerosols

sourced directly from the ocean surface, may be an important aerosol source over the

majority of Earth's surface (Lewis and Schwartz, 2004). The formation of SSA results

from wave breaking on the surface of the ocean. Wind over the ocean surface in excess of

5 m/s produces breaking waves and the formation of whitecaps (de Leeuw et al, 2011).

When a wave breaks, air bubbles are entrained in the subsurface of the ocean, which then

rise to the surface and burst. The bursting bubbles eject small droplets into the atmosphere

that can evaporate when exposed to a relative humidity < 70-74% and form primary

particles sourced from the ocean water (Blanchard et al, 1989). Two distinct

Figure 2.1   The production of droplets from bubble bursting at the surface of the ocean. The differences in the production mechanisms are shown, as well as an indication of the differences in the number of droplets produces. Adapted from (Resch et al., 1986).

mechanisms for SSA production occur as the result of bubble bursting, called film drops and jet drops (Blanchard, 1954), as illustrated in Figure 2.1. The bubble film cap that is exposed to the atmosphere can rupture, ejecting hundreds of small droplets upward. Particles formed by this mechanism are film drops. Additionally, after a bubble bursts, water quickly fills in the air cavity left behind by the bubble, propelling a small jet of water into the atmosphere. The resulting water jet, which is typically 5-10% of the thickness of the bursting bubble's diameter, can break apart into several droplets, or jet drops (Blanchard, 1963).

The magnitude and size of SSA produced by these two droplet types is heavily dependent on the size spectra of the originating bubbles (Deane and Stokes, 2002). Smaller bubbles are associated with more efficient production of jet drops, while film drops are produced exclusively by larger bubbles. For example, Wu (1988) observed that bubbles smaller than 2mm in diameter exclusively produce jet drops, while larger bubbles are more effective at producing film drops. Furthermore, it is important to note that the number of drops produced by film and jet drops differ significantly. Jet drops, which are larger in size compared to film drops, were suggested by Blanchard (1989) to contribute the majority of

the mass of SSA, while film drops, which are smaller in size but are produced in much

greater numbers, were estimated to dominate the contribution to total particle number

(Blanchard, 1989). Further research confirms that the smaller SSA are most prevalent in

terms of particle numbers and that their influence to SSA mass is negligible (O'Dowd,

2004). Therefore, the majority of emitted SSA mass results from the particles in the larger

end of the size distribution, formed from jet drops, whereas the film drops are responsible

for the greatest production of particle numbers.

In addition to bubble size, other factors that can affect the production flux and size

distribution of SSA from bubble bursting include temperature and surface tension.

Temperature changes alter the viscosity and thus the bursting dynamics of the bubble

films. Increased surface tension, which is influenced by the presence of surface active

materials that preferentially accumulate on the ocean surface, can suppress bubble bursting

processes and affect the size, number, and composition of the resulting SSA particles

(Lewis and Schwartz, 2004; Modini et al., 2013). The role of surface active materials on

the composition of nascent SSA holds considerable relevance to the research presented in

this thesis; a more detailed explanation of these effects is given later in this chapter in the

discussion on the Sea Surface Microlayer (Section 2.3).

2.2 SSA Size

Direct measurements of ambient SSA over the surface of the ocean show that primary sea

spray particles are emitted in all size modes, ranging from a few nanometers to tens of

micrometers in diameter (Clarke et al., 2003); however, the majority of the aerosol number

produced dominate in the sub-micrometer size range (Blanchard et al., 1989, Bates et al., 1998, Prather et al., 2013). Clarke et al. (2003) further observe from SSA measurements that the smallest of the submicron particles, between 0.03 – 0.40 microns, have the highest peak in number concentration.

Similar to other types of aerosol in the atmosphere, the size of a sea spray particle governs its behavior in the marine boundary layer. First, the direct and indirect radiative effects depend on aerosol size distributions. As previously discussed, aerosol size controls the scattering and absorption potential in the atmosphere (Seinfeld and Pandis, 2006; Bates et al., 1998). Likewise, the size of a particle has an important influence on its cloud nucleating properties. From equation 1.4 (Section 1.3), it becomes apparent that a larger dry particle diameter requires a lower supersaturation to activate as cloud droplet, hence it is easier for larger particles to act as CCN under atmospherically relevant supersaturations. Additionally, particle size is also influential on the atmospheric lifetime of the particle. The fate of supermicron particles is rapid deposition back into the ocean surface (Cunliffe et al., 2013), because larger particle diameters are more prone to settling out by dry deposition (Seinfeld and Pandis, 2006). The submicron particles, which are able to be lifted aloft after emission, have longer atmospheric lifetimes and are therefore more influential on climate relevant processes in the atmosphere, such as the direct and indirect effects (Tsigaridis, 2013).

2.3 The Sea Surface Microlayer

The SML is a thin layer, operationally defined between 1- 1000 μm, on the ocean surface that differs in composition and physio-chemical properties to underlying waters (Cunliffe et al., 2013). The SML consists of a complex mixture of dissolved and particulate organic compounds sourced from phytoplankton blooms and elevated microbial activity in surface ocean waters. Figure 2.2 depicts the relationship between the SML and biological activity in the ocean. The biogenic compounds comprise many different types of organic molecules with different properties, including polysaccharides, lipids, amino acids, and proteins. Typically, the SML is enriched in organic compounds with respect to subsurface water because they are surface active and have low solubility, which causes them to preferentially accumulate at the surface. Wurl et al. (2011) observed that the concentration of organics in the SML is typically greater than in bulk seawater for nearshore, offshore, and oceanic locations. Furthermore, the SML is ubiquitous across ocean surfaces and forms the interface of ocean- atmosphere interactions. Hence, the SML is likely important for controlling exchange processes between the oceans and the atmosphere. For example, the SML is suggested to act to dampen capillary waves, influence exchanges of gasses in and out of ocean water, and suppress bubble bursting processes (Lewis and Schwartz, 2004; Cunliffe et al., 2010).

Similar to SSA production, the formation and persistence of the SML can be attributed to bubble processes in the surface of the ocean. In the same manner that partitioning occurs at the ocean surface, surface active compounds preferentially accumulate at the interface of submerged air bubbles as they rise. The rising bubbles then transport these compounds
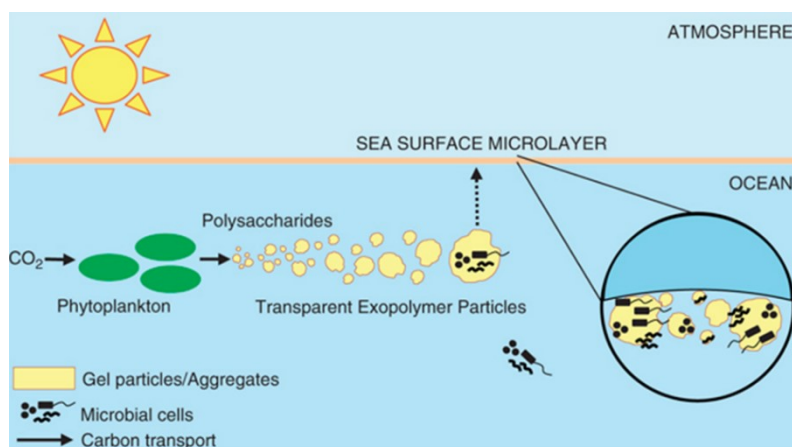
Figure 2.2   An illustration of the sea surface microlayer and the source of organic enrichment at the ocean surface. Adapted from (Cunliffe et al., 2009).

to the ocean surface. This process, which results in an enrichment of the surface active organic compounds in the SML, is called bubble scavenging. Previous studies give strong evidence of the bubble scavenging mechanism. A laboratory study identified that organic surfactants 'out compete' more soluble components at bubble interfaces in a solution and bring them to the surface (Chingin et al., 2016). Surfactant scavenging by bubbles has also

been well characterized in sparkling wine and contribute largely to the release of flavor and aromas in champagne (Liger-Belair, 2009). Also, water treatment plants rely on bubble scavenging to remove organic compounds in waste water (Khuntia et al., 2012). Additionally, results from field investigations suggest scavenging occurs in the ocean; after events of high wind speeds over the ocean, which entrain air bubbles in the subsurface due to breaking waves, increased enrichment of organic compounds on the surface have been observed. (Cunliffe et al., 2013; Wurl et al., 2011).

The mechanisms contributing to increased organic enrichment in the SML also provide the necessary conditions for primary SSA production, which suggests there is a direct link

between the SML and the composition of SSA. A variety of field and laboratory studies

provide evidence to support this hypothesis. First, CCN measurements in a laboratory

have shown that the presence of a surfactant in a bubbled solution decreases the

hygroscopicity of the resulting particles due to an increase in organic composition

compared to a surfactant-free solution (King et al., 2012). Additional bubble experiments

in a laboratory show that the particles are enriched in organic composition relative to the

concentration of organics in the bulk solution, as shown in Figure 2.3 (Chingin et al.,

2016). In the field, researchers have found a high occurrence of organic compounds in

nascent SSA (Quinn et al., 2014), and another study concludes that certain organic

constituents in SSA were sourced directly from the SML (Russel et al., 2010). Therefore,

it is reasonable to infer that a portion of the organic component in SSA formed by bubble

bursting stems from the organic enrichment in the SML. The extent to which the SML

influences SSA composition, however, is poorly constrained and requires further research

to improve our understanding of the climate impacts of SSA (Quinn et al., 2015).

The SML has further influence on SSA production and composition by affecting the

dynamics of bursting bubbles. Under conditions of higher surfactant concentrations on the

ocean surface, bubble-bursting processes are suppressed, allowing bubbles to exist longer

before rupturing (Sellegri et al., 2006). Persisting surface foams have been reported in

bubble diffuser experiments with solutions containing surfactants because of bubble

bursting suppression (King et al., 2012). During the extra time that the bubbles persist in

the presence of surfactants, the more water-soluble dissolved compounds can drain off the

bubble films while the insoluble species remain. Then, upon bursting of the bubble, the

insoluble compounds are able to be ejected to the atmosphere as film drops (Modini et al.,
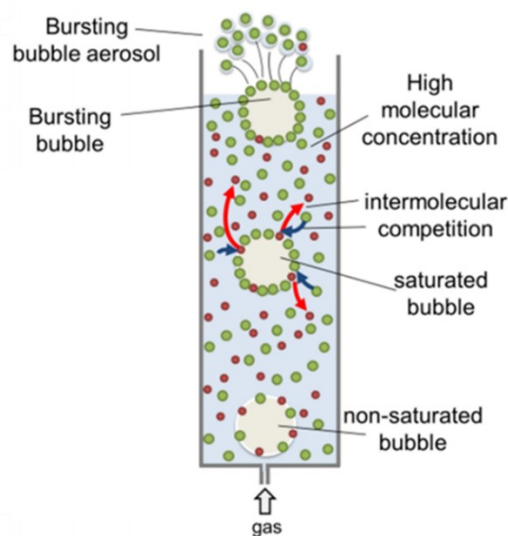
Figure 2.3   Diagram showing the enrichment of organics in aerosols formed from bubble bursting processes compared to the inorganics. Adapted with permission from (Chingin et al., 2016). Copyright 2016 American Chemical Society.

2013). Further examination of bubble draining demonstrates that inorganic ions, as well as soluble organic compounds, preferentially drain from bubble films when higher concentrations of surfactants are present, and the organic surfactants that remain on the bubble film are more abundant in SSA (Frossard et al., 2014). Similarly, the production and evolution of sea foams resulting from wave breaking can have an effect on the aerosol production. Modini et al. (2013) also report thinning of the bubble films after extensive draining due to the presence of surfactants, and observe a decrease in the production flux of SSA as a result. Therefore, the role of bubble processes in the ocean surface on the formation of SSA and the SML suggests an important connection between the SML and the composition of SSA.

2.4 SSA Composition

Seawater is a highly concentrated solution of dissolved salts and organic material from biological processes in the ocean. Table 3.1 (Section 3.3.1) provides a summary of the major dissolved inorganic ions in seawater and their typical concentrations. In terms of the organic material, phytoplankton exudates are the dominant source of dissolved organic matter (DOM) in the ocean (Nagata, 2003). As SSA are formed directly from seawater, they consist of particles with both organic and inorganic compositions.

Similar to particle size and number flux, there is a direct connection between the production mechanism of SSA and the composition of the resulting aerosol. As a result, the composition of the particle has a strong dependence on size. Specifically, supermicron SSA have been found to consist primarily of sea salt, and the organic fraction becomes more prominent as particle diameter decreases (O'dowd, 2004, Collins et al., 2013). Results of a previous study show the largest changes in organic fraction are observed at the smallest particles size ranges; submicron particles with a diameter of 40 nm were found to have an organic fraction of 80%, compared to 40% observed for 100 nm diameter particles (Quinn et al., 2014).

Larger particles account for the majority of the particle mass, providing a bias of total SSA composition fraction to the inorganic component. However, due to their greater number concentrations, the composition of the submicron SSA is highly relevant in the atmosphere. Fitzgerald et al., (1991) found that submicron particles account for 90% of particle number and only 5% of particle mass. Furthermore, the transfer of organics from

seawater to primary SSA is selective toward organic compounds with a certain set of physicochemical properties, typically surface active molecules of biological origin (Schmitt-Kopplin et al., 2012). As the organic fraction of SSA dominates in the size range where particle number is most significant, particles have longer residence times, and particles are most influential on climate processes, the influence that the organic component has on SSA is crucial.

2.5 Review of the Significance of SSA

The importance of SSA in the atmosphere has been thoroughly discussed in scientific literature. SSA are estimated to have an important contribution to the total aerosol mass emitted to the atmosphere each year. The total atmospheric mass loading of SSA is estimated to be $2 \times 10^{12} - 2 \times 10^{14}$ kg yr^{-1}, similar in magnitude to the mass loading of mineral dust aerosols (Fitzgerald et al., 1991). The large range in the estimated SSA mass flux poses a challenge to the modelling community in capturing a representative SSA flux (Grythe et al., 2014). In fact, SSA has the largest uncertainty in atmospheric mass flux, which is greater than the uncertainty for all other aerosol sources combined (Textor et al., 2006). Despite a variety of efforts in field, laboratory, and modelling studies, the current flux estimates of SSA are poorly constrained and continue to be an area of ongoing research (Lewis and Schwartz, 2004; de Leeuw et al., 2011). Nevertheless, studies have identified that SSA constitute one of the largest natural aerosol sources and play a key role in atmospheric processes, specifically in the marine boundary layer where continental influences are limited (O'Dowd et al., 2004, 2007).

Previous observations suggest that SSA have a significant contribution to the direct effect in the atmosphere. Measurements of ambient particle sizes in the remote Southern Ocean and Pacific Ocean have demonstrated that the peak in the size distribution of SSA particles occurs below 1 μm, making them highly relevant for efficient scattering of shortwave radiation (Bates et al., 1998; Clarke et al., 2003). Representative ocean waves generated in a laboratory confirm that primary SSA emissions fall within the same size range (Prather et al., 2013), further confirming the importance of SSA on the direct effect. While less efficient than the sub-micrometer SSA particles, SSA particles in the supermicron size range can also contribute to the direct effect due to the deviation from spherical shapes that increase their scattering ability (Chamaillard et al., 2006), and the larger mass contribution of SSA > 1 μm provides additional compensation for the less efficient scattering (Kleefeld et al., 2002). As such, SSA are the most influential particle source in terms of the direct effect in the marine boundary layer and may comprise the largest natural aerosol contribution to global direct radiative effects (Quinn et al., 2015).

In addition to direct radiative effects, SSA can act efficiently as CCN as well. Since SSA are emitted in remote locations where the background is considered clean, SSA are likely to be relevant for the indirect effect in the marine boundary layer in open ocean regions (Quinn et al., 2015). Ambient observations by Leck and Bigg (2005) suggest that SSA are a dominant source of CCN in the remote marine boundary layer. Likewise, a study by Orellana et al. (2011) demonstrates the presence of SSA in arctic clouds and fog. Under clean conditions, small changes in the concentration of CCN can have important effects on the radiative properties of the cloud (Murphy et al., 1998). As a result, a better understanding of SSA may resolve key areas of uncertainty in the representation of the

indirect effect in climate projection models (Quinn et al., 2015; IPCC). Since Aitken and accumulation mode particles, especially between 0.030 – 0.40 µm (Clarke et al., 2003), account for the majority of particle number emissions from SSA, are highly active in climate relevant processes, and consist of 40-80% organic material (Quinn et al., 2014), understanding the role that organic material in SSA emissions in the marine boundary layer have on CCN processes is important. Organics are have been identified to lower the hygroscopicity of SSA during mesocosm experiments (Collins et al., 2013), and artificial seawater containing organics were found to have a decrease in CCN activity compared to seawater solutions without organics, suggesting the presence of organics cause a reduction in CCN activation in primary particles (Fuentes et al., 2010). Despite these previous studies that have aimed to characterize the influence of SSA composition on hygroscopicity, the overall effect of organic composition on CCN activity in SSA remains unresolved.

2.6 Summary

Given the large number concentrations of SSA emitted at CCN relevant sizes, organics dominating the composition of the particles at these sizes, the large percentage of ocean coverage on Earth, and previous evidence that SSA are dominant in the marine boundary layer, resolving the hygroscopicity of marine organics in SSA is important for improving our understanding of the aerosol indirect effects, and the ability of organics to activate as cloud droplets in the atmosphere is poorly constrained (IPCC, 2013). Therefore, in this thesis, the effect of organic composition on the hygroscopic properties of primary SSA is investigated using real surface seawater samples, with a focus on characterizing the SML

and bulk subsurface water, as the influence of organic composition in sea spray particles on cloud formation in the marine boundary remains inconclusive. A new laboratory method is developed to process seawater samples prior to instrumental analyses to permit the characterization of the hygroscopicity parameter, κ, of marine organic compounds using the volume fraction mixing rule outlined by κ-Köhler theory. The process of developing the method is discussed in detail, as well as its validation using control solutions. Then, the technique is applied to surface ocean water samples, and the hygroscopicity of generated particles are measured. Given the evidence that the SML is influential in SSA composition, samples of SML and bulk subsurface water are compared to assess the role of the organics in SML and bulk water. Lastly, I present results and scientific questions that have been raised using the new method and discuss the influence of physical and chemical mechanisms to explain our observations.

CHAPTER 3   METHODS

Chapter 3 presents the methods used for the scientific analysis in this thesis. A general overview of the method used to analyze the samples is given, and additional background information is provided for each aspect of the experimental method: field sample collection, sample processing using dialysis, instrumental analysis, and determinations of κ.

3.1 Sample Analysis

SML and bulk water samples were collected from a small boat in the Northwest Arm in Halifax, NS. Bulk water, defined as subsurface water below the SML, was collected at a depth of 1 m using a peristaltic pump. The SML was sampled using the glass plate dipping technique. All sampling materials, including the glass plate, neoprene squeegee, funnel, tubing, and collection bottles, were cleaned with isopropyl alcohol and rinsed thoroughly with seawater in situ prior to use. Gloves were worn during sampling, and caution was taken to avoid touching the clean sampling surfaces to prevent contamination; two people were involved to use a "clean hands – dirty hands" sampling approach. In addition, sampling was carried out the downwind side of the boat such that the boat was drifting into clean, undisturbed SML. GPS coordinates, wind speed, and ocean surface conditions, such as slick or non-slick conditions, were also recorded during sampling. Slicks are regions where dampened capillary waves can be detected visually and occur when the organic surfactant concentration in the SML passes some unknown threshold (Wurl et al., 2011). The samples were immediately placed in a cooler of ice after collection to limit

temperature and photo degradation of sensitive organic constituents (Chen and Wangersky, 1996). Finally, the samples were taken to a laboratory and stored in a refrigerator before processing.

In the lab, each sample was processed using dialysis to reduce the concentration of inorganics before analysis. The sample to be dialyzed was poured into a tube of the dialysis membrane (Spectrum Laboratories 131060). Both ends of the membrane were sealed, and the tubing was placed inside of a 1 L beaker filled with deionized water, the dialysate, to begin dialysis. A peristaltic pump (Greylor R120180) capable of pumping 1 L min^{-1} was used to circulate deionized water from a reservoir into the dialysis beaker. The pump, controlled by a timer, completely replaced the dialysate in the beaker with deionized water once per hour, preventing an equilibrium from being achieved between the sample and the dialysate. Overflow from the beaker was collected in a catchment basin. Periodically, the deionized water reservoir was refilled and the catchment basin was emptied. The entire setup, as shown in Figure 3.1, was carried out in a refrigerator to keep the seawater in the dark and below 4°C to limit the biological and photo degradation of sensitive organic components (Chen and Wangersky, 1996).
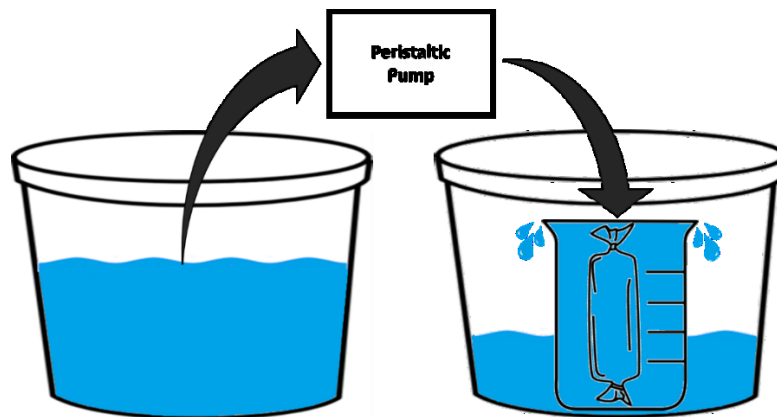
Figure 3.1   Schematic diagram of the dialysis setup used in a refrigerator.
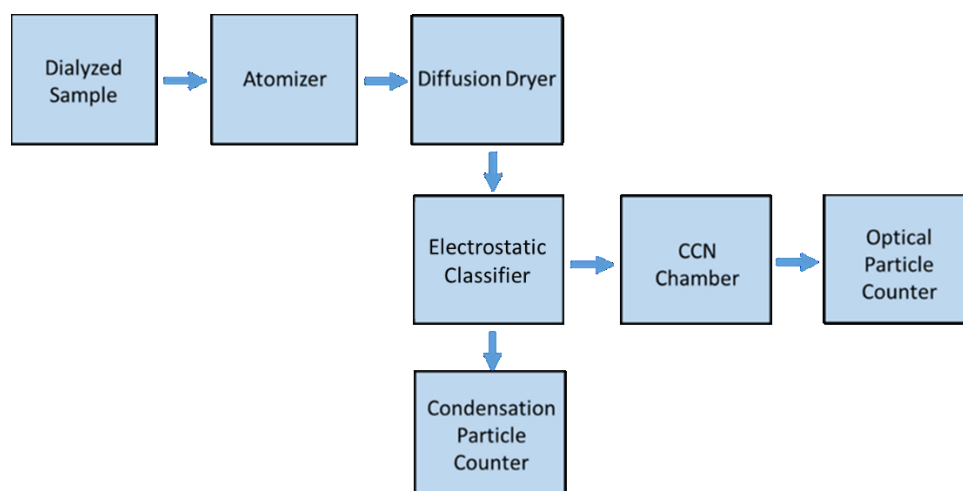
Figure 3.2   Block diagram of the instrumental setup used for the analysis of seawater
samples before and after dialysis.

Once the samples were collected and dialyzed, they were analyzed for their hygroscopic

parameter using the instrumental setup shown in Figure 3.2. Using an atomizer, particles

were generated from the samples and dried in a diffusion dryer to form dry particles.

Several precautions were taken to ensure measurement accuracy. The atomizer was

disassembled and cleaned between sample solutions, and particle counts were measured

from atomized deionized water solutions to ensure no impurities were present. The

generated aerosol was then passed through an electrostatic classifier (TSI 3082) with a

differential mobility analyzer (DMA) (TSI 3081) to size select particles based on mobility

diameter. While some degree of particle loss is inevitable due to diffusion, conductive

tubing was used in the plumbing to minimize particle loss due to charge interactions with

the walls of the tubing after the particles were charged in the electrostatic classifier. The

resulting monodisperse aerosol from the DMA was directed to a condensation particle

counter (CPC) (TSI 3772) to provide accurate counts of particle number concentrations.

The flow from the DMA was also sampled by a CCN chamber (DMT CCN-100), where

particles were subjected to controlled supersaturations to induce cloud droplet formation.

The cloud chamber was calibrated using an ammonium sulfate solution to attain the effective supersaturation in the column used in subsequent calculations. The number of particles that activated as cloud droplets was then counted using an optical particle counter at the bottom of the CCN chamber.

The data obtained from the instrumental setup provides quantitative measurements of the fraction of CCN that activate at a given dry particle diameter and supersaturation. Using κ–Köhler theory, the hygroscopicity parameter of the particles can be inferred from these data using activation curves obtained from scans of dry particle diameter at a constant supersaturation. In addition to hygroscopicity measurements, analytical methods for ion chromatography (IC) and a dissolved organic carbon (DOC) measurements were employed to characterize the salinity and DOC concentration in the seawater samples, respectively. By applying a simplifying assumption to the particle compositions, the quantification of chemical concentrations in the seawater samples permits the hygroscopicity of the marine organics to be determined using the volume fraction mixing relationship outlined by κ–Köhler theory. A further discussion on the function of each instrument used and the approach and assumptions used for inferring hygroscopic measurements is provided below.

3.2 Sample Collection

The primary objective of this thesis is to investigate the role that marine organics have on the hygroscopic properties of primary SSA emissions. As a secondary objective, the differences between the organic components in the SML are compared to bulk subsurface

water. To address these research questions, it is necessary to collect concurrent samples of the SML and bulk water in the field. While bulk water collection is a relatively straightforward process, collecting the SML requires special techniques. The glass plate sampling technique was selected for SML sampling during this project. The advantages, disadvantages, and sampling routines for collecting the SML using a glass plate are discussed below.

The glass plate sampler was originally designed to collect low volume SML samples. The principles of operation are simple: the glass plate is dipped into the water perpendicular to the surface and removed at a slow, steady rate. The plate provides a hydrophilic surface for the SML to adsorb, allowing for subsequent collection using a neoprene squeegee, a funnel, and a bottle (Harvey and Burzell, 1972). The dipping process is then repeated until a desired volume of sample is collected.

While there are other methods for sampling the SML, the glass plate has several advantages to the objectives of this study. Correct execution of the sampling mechanics provides repeatable results of SML thickness as opposed to other sampling methods. Likewise, the thickness of the SML sampled using a glass plate is thinner than other types of sample collection. As a result, utilizing the glass plate method collects samples with higher enrichment of surface active organic composition from the SML, likely a result of less dilution with subsurface water. Furthermore, the collection of a thinner sample is thought to be more selective of biological compounds, especially products of microbial activity. The glass plate method is also more robust than other methods for collecting organic compounds as it is non-discriminatory to specific types of microbes or microbial

products. In addition, certain lipids and amino acids, which are highly hydrophobic, readily absorb to the glass plate during sampling. Generally, as compounds tend to be more hydrophilic, they are less likely to be selected for by glass plates (Cunliffe and Wurl, 2014). As such, the glass plate method is most suitable for collecting SML field samples in this study due to the focus on marine organic compounds.

The glass plate sampling method also has some drawbacks that could provide bias in the samples. While thinner microlayer is beneficial for collecting biological organic surfactants, it may only collect a sample that is representative of the upper most level of the SML, which may not include changes in properties previously found in the lower levels of the microlayer (Zhang et al., 2003). The time scale required to collect a sufficient amount of samples can have undesirable effects on the integrity of the sample. Specifically, certain amino acids found in the SML are highly reactive and can change significantly in abundance during sample collection and storage. In addition, glass plates have trace amounts of inorganic impurities fused into their structure (ppb to ppm) which are capable of leaching into collected samples (Ebling and Landing, 2014).

3.3 Analysis Techniques

3.3.1 Dialysis

For the purpose of measuring the hygroscopicity parameter of only the organic constituents in seawater, the dissolved inorganic components need to be removed from the sample prior to analysis. During the process of removing the dissolved salts, the integrity

of the organics must also be maintained to ensure the experimental results are representative of the environment where the sample was collected. To that end, dialysis was chosen as a suitable desalting method as it is simple to perform and the process can be controlled in a manner to limit the degradation of sensitive marine organics. The following discussion provides an overview of the principles of dialysis and describes the dialysis method used in the experiments presented in this thesis.

Dialysis is a laboratory technique used to physically separate dissolved compounds in a solution by using a porous, semipermeable membrane. Typically used for sample purification in biological applications, dialysis has been established as an effective way to remove unwanted constituents from a sample while components of interest are conserved (e.g. Haririan et al., 2010; Ungaro et al., 2012). During dialysis, a sample solution is placed inside a tube of dialysis membrane that is then placed in a reservoir filled with a buffer solution, called a dialysate. Molecular diffusion occurs in the sample, allowing dissolved constituents to pass through the pores of the dialysis membrane into the dialysate (Figure 3.3). Two key criteria are necessary for laboratory dialysis to be an effective mechanism for separating dissolved components in a sample solution: the sample must contain constituents of variable sizes, and a concentration gradient must be present between the sample and the dialysate. Other factors that can influence the dialysis process include temperature, reservoir and sample volume, sample concentration, membrane surface area, and the dialysate used.

In order to achieve physical separation, dialysis membranes have a defined pore size, called a molecular weight cut off (MWCO). The MWCO specifies a size range of the
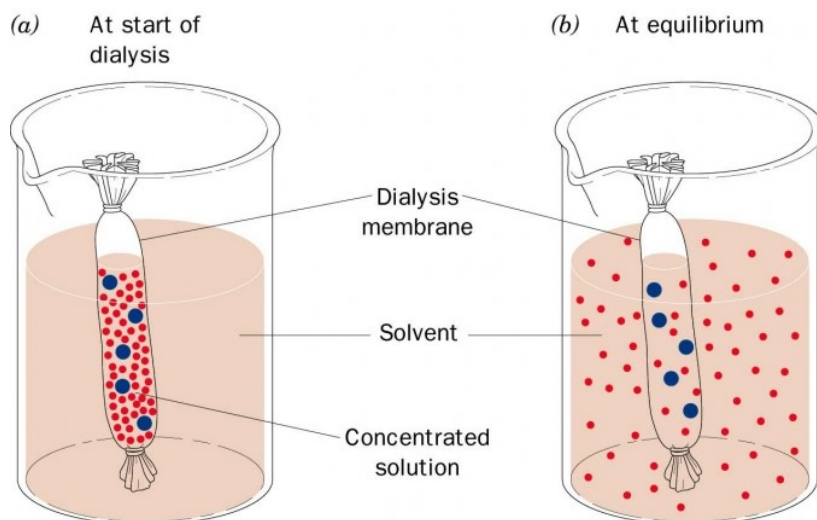
Figure 3.3   Diagram depicting laboratory dialysis used for desalting. The red dots
              represent the dissolved inorganic salts in seawater, and the blue dots signify
              marine organic compounds. The dialysis membrane is a tube that can be
              sealed with a seawater sample solution inside and placed inside a reservoir
              filled with deionized water. Diffusion will continue until an equilibrium is
              reached between the solute concentration in the sample and reservoir
              solutions. Adapted from (Voet and Voet, 2011).

dissolved constituents, by molecular mass, which are able to permeate through the pores

of a dialysis membrane. Therefore, the components that are to be preserved in the sample

must have a higher molecular weight than the compounds which are to be removed, and

the dialysis membrane must have a MWCO which corresponds to these sizes. The size of

the individual pores of a membrane vary, which explains why the MWCO of a membrane

is defined by a range. During dialysis, a concentration gradient drives molecular diffusion

through the membrane. In a solution, the dissolved components preferentially diffuse from

areas of high to low concentration. By placing a sealed tube of dialysis membrane that

contains a solution with a high dissolved solute concentration inside of a reservoir solution

with a lower solute concentration, a concentration gradient is achieved and diffusion

Table 3.1   The concentrations of major dissolved ions in seawater with a salinity of 35 ppt. The average seawater contains 35 g of salts per liter. The composition of inorganic mass is dominated by NaCl. In total, Na^+ and Cl^- ions comprise more than 86% of the mass of dissolved ions in seawater. Data obtained from (Pilson, 2013).

Dissolved Ion	g kg^{-1}	mM
Na^+	10.781	480.57
K^+	0.399	10.46
Mg^{++}	1.284	54.14
Ca^{++}	0.4119	10.53
Sr^{++}	0.00794	0.0928
Cl^-	19.353	559.4
$SO_4^=$	2.712	28.93
HCO_3^-	0.126	2.11
Br^-	0.0673	0.865
$B(OH)_3$	0.0257	0.426
F^-	0.0013	0.07
Total	**35.169**	**1147.59**

through the membrane is favorable. The components that are small enough to pass through the membrane can be removed, while the larger constituents are retained in the sample.

The variability between the molecular weight of the organic and inorganic components of seawater and the high concentration in seawater satisfies the necessary conditions for laboratory dialysis to be used to desalt the seawater. A summary of the concentration of the major dissolved inorganic ions is given in Table 3.1. The molecular weights for the inorganic ions range from 18.998 – 98.063 g mol^{-1} (F^- and SO_4^{2-}, respectively). A study by Moore et al. (2008) reports the estimated average molecular weight of DOM from the Atlantic Ocean in Gulfstream and estuarine seawater to be 4370 and 4340 g mol^{-1}, respectively. Given the lower molecular weights of the inorganic constituents of seawater

compared to the organic components, the technique of dialysis applied to a seawater sample could be a suitable method for removing the seawater while retaining the organic composition. In order to achieve the research objective discussed in this thesis, the amount of dissolved salts should be removed as much as possible to completely isolate the organic constituents. A dialysis membrane with a MWCO of 100-500 Da (Spectrum Laboratories 131060) was selected, as this MWCO would permit the low molecular weight inorganic ions to be removed while most of the organic components remain in the sample.

A series of tests were conducted on NaCl solutions and filtered seawater to develop the dialysis method utilized for processing seawater samples in this thesis. Once initial tests verified that dialysis was capable of desalting solutions as concentrated as seawater, additional tests were carried out to characterize the influence of dialysate volume, turbulence, and temperature on the time efficiency and effectiveness of desalting. Additionally, experiments were performed for quantitative analyses of organic retention during dialysis. Further information about the tests used to develop and characterize the dialysis method is located in Appendix B.

3.3.2 Particle Generation

There are a variety of methods available for generating aerosols in a laboratory, including bubble diffusers, plunging jets, artificial waves, and atomizers. Comparisons of the generation methods demonstrate that different modes of particle generation result in significant differences in the resulting aerosol size distributions and aerosol properties (Fuentes et al., 2010; King et al., 2012). In addition, most mechanisms fail to reproduce

the bubble size distributions in real breaking waves in the ocean, hence the size distributions of the particles produced are not representative as well (Prather et al., 2013). The challenge in reproducing particles characteristic of ocean processes can complicate analyses of laboratory generated SSA.

For the research objectives in this thesis, atomization was selected as an appropriate method for particle generation. An atomizer works based on Bernoulli's principle and uses a recirculation system from a solution reservoir. Filtered compressed air flows through a critical orifice into the chamber of the atomizer, which causes water from the solution reservoir to be drawn up through a feed tube. Upon contact with the air jet, the solution from the feed tube is atomized into a series of droplets. The larger droplets collide with the walls inside the chamber and drain back into the solution reservoir. Smaller droplets are pushed out of the exit on the top of the chamber. Once the droplets leave the atomizer, the excess water is removed by passing the droplet flow through a diffusion dryer. The diffusion dryer consists of an inner mesh tube surrounded by silica desiccant gel. The desiccant lowers the relative humidity inside the dryer such that the water evaporates and the droplets effloresce; as a result, a distribution of dry particles with the composition of the dissolved constituents in the sample solution are formed. Figure 3.4 illustrates the instrumentation used for this mechanism of particle production.

The mechanism of generating particles from an atomizer differs substantially from the bubble bursting processes in the ocean. As the bubble bursting process shows selectivity in partitioning certain compounds into the aerosol phase, the composition of the particles shows a strong correlation with particle size, as previously discussed (e.g. O'Dowd et al.,
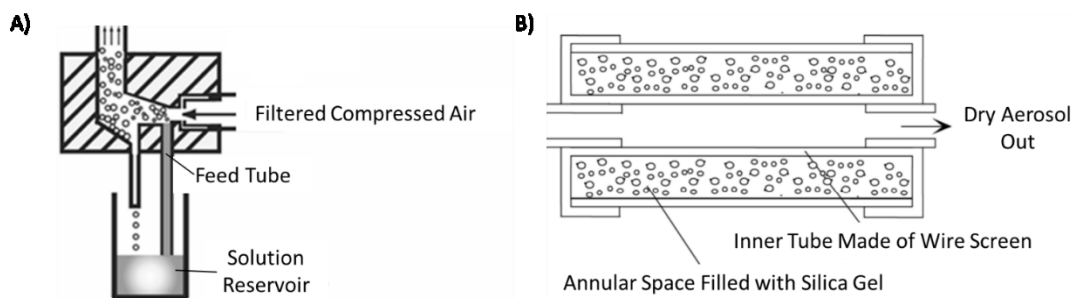
Figure 3.4   Schematics of the particle generation instrumentation. Adapted from (Lu et al.,1999) and TSI Inc. (A) identifies the main components of an atomizer and their function. (B) illustrates the interior of a silica gel diffusion dryer. Copyright 2017 TSI Incorporated, used with permission.

2004). In an atomizer, however, it is commonly assumed that particle composition does not change as a function of size (Petters and Petters, 2016; Prisle et al., 2010). Instead, the mechanics of particle formation in an atomizer suggests that the composition of the particles that form reflect the composition of the dissolved ions in its sample solution, assuming that all the ions are diffuse in the solution. This characteristic of an atomizer is advantageous to our analysis; the salinity and dissolved carbon content can be quantified in the seawater samples, and according to this assumption the mass fractions of the organic and inorganic components in the particles will reflect these values.

3.3.3 Particle Size Selection

After the dry particles leave the diffusion dryer, they enter the electrostatic classifier to be size selected by the DMA. By using electrical mobility, the DMA used in this thesis is capable of size selecting particles between 10 nm – 1 µm from a polydisperse aerosol distribution. This method for separating particles of different sizes based on electrical

charge was first described by Hewitt (1957), and it is now widely used among aerosol scientists.

Before the particles can be size selected based on their electrical mobility, they need to be charged. The particles are given a known charge distribution by passing through a neutralizer, which in this case was a soft x-ray source (TSI 3088). Once the particles are charged by the x-ray source, the polydisperse flow is directed through the DMA to be size selected. The DMA is a hollow cylindrical column with an electrode in the center. An electric potential between the electrode and the electrically-grounded outer wall of the DMA creates an electric field inside the chamber. A laminar sheath flow of particle-free air flows continuously through the column, and as the particles enter, they are carried by the sheath flow through the electric field. Since the particles are charged, they interact with the electric field, causing them to be attracted to the central electrode. Their electrical mobility, which is dependent upon their size and charge, determines the degree of attraction the particles experience toward the electrode. Smaller particles have a higher electrical mobility; thus, they are more attracted to the central electrode than larger particles. There is a small slit in the electrode in the bottom of the column that particles with a narrow range of electrical mobility, and hence size, are able to pass through when a given voltage is applied to the electrode. Smaller particles get stuck to the electrode, and larger particles will pass by the slit. As a result, the aerosol that exit through the slit are monodisperse, or exist at one size called a mobility diameter (Figure 3.5). By varying the voltage of the central rod, it is possible to select the mobility diameter of the resulting monodisperse aerosol.
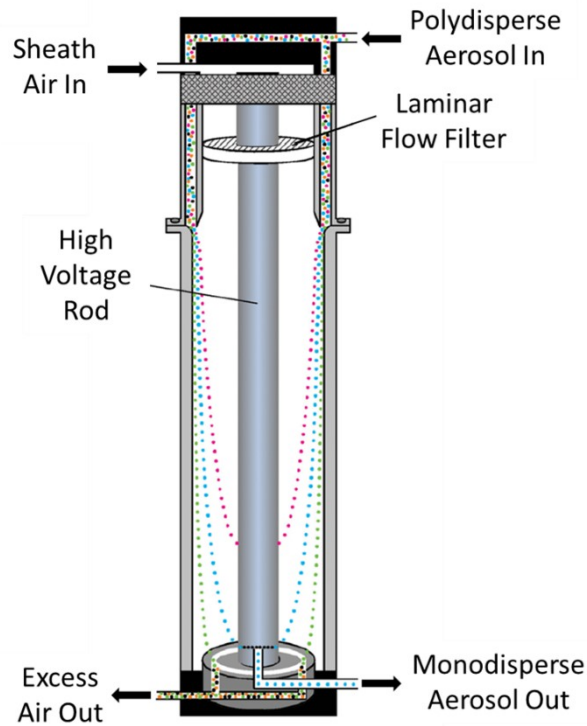
Figure 3.5   A diagram showing the mechanism of particle size selection inside a DMA. The light blue, red, and green lines show the behavior particles with different electric mobilities. Only particles with the narrow range of electric mobility associated with voltage of the center rod will pass through the slit at the bottom of the DMA (blue line), forming a monodisperse particle distribution. Copyright 2017 TSI Incorporated, used with permission.

3.3.4 Particle Counting

The flow of the monodisperse aerosol then moves from the DMA to a CPC (TSI 3772) to be counted. Typically, obtaining accurate counts of submicron aerosol number concentrations is a challenge because the particles are too small to be detected reliably using optical methods. To resolve this issue, the CPC is able to provide accurate counts of particles in submicron size ranges by growing the particles before counting. Using a heated chamber, the CPC vaporizes a source of butanol and introduces it into the aerosol

flow. The particles, now in the presence of the saturated butanol vapor, then enter a cooled condenser. The drop in temperature supersaturates the butanol vapor, causing it to condense onto the aerosols. As a result, the particles grow quickly to larger sizes, where they are counted optically by light scattering. The instrument is capable of counting aerosol number concentrations as high as 10^4 cm^{-3}.

3.3.5 CCN Activation

The monodisperse aerosol flow that exits from the DMA is also split to a CCN Chamber (DMT CCN-100). The CCN chamber subjects the particles in the aerosol stream to supersaturated conditions to simulate cloud droplet formation. The cloud chamber is a cylindrical column that uses a water supply and heat to control the supersaturation within. On the inside walls of the chamber, a wetted liner receives a constant supply of moisture from an external water reservoir. The outer chamber wall is also equipped with heaters, which heat the chamber from the outside. Since the rate of water vapor diffusion is greater than the diffusion of heat, the instrument takes advantage of the different diffusion rates to produce supersaturated conditions in the center of the chamber. At the chamber wall, the air is saturated with respect to water vapor due to the wetted lining, and the water vapor from the chamber perimeter disperses toward the center of the column faster than the heat. Therefore, as the water vapor moves toward the center of the column where the temperature is cooler than the outer perimeter, water vapor is supersaturated because the saturation of water vapor is dependent upon temperature. The degree of supersaturation increases from the outer walls to the center, where a zone of maximum supersaturation is

achieved. By controlling the temperature of the heaters, the maximum supersaturation in the center of the column can be controlled.

The particle stream is introduced in the center of the column, and a laminar flow of sheath air through the chamber causes the particles to remain in the center. As a result, the particles are subjected to the maximum supersaturation in the chamber. During this time, the particles that are able to serve as CCN at the specified supersaturation will rapidly take up water and form cloud droplets. An optical particle counter located after the cloud chamber counts the cloud droplets upon exit. The optical particle counter will only count the particles that activate and grow to micrometer sized droplets; unactivated particles pass
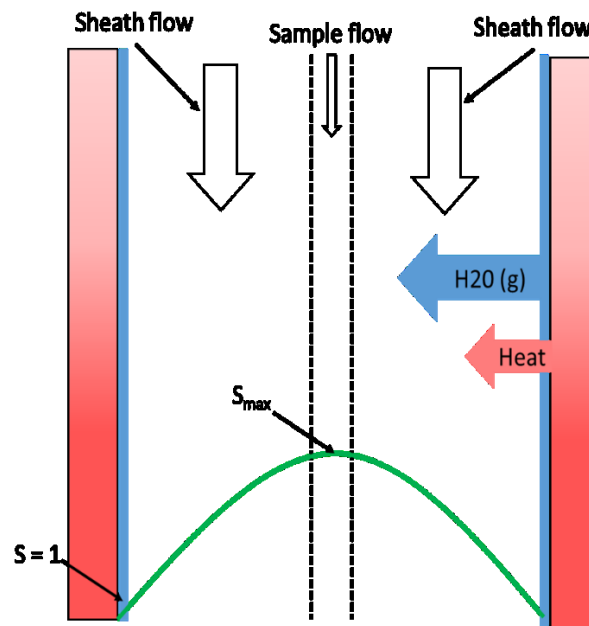
Figure 3.6   A graphical depiction showing how supersaturation occurs inside the cloud chamber. The diffusion of water vapor occurs faster than heat toward from the walls to the center of the column. The green line represents supersaturation in the chamber, which increases with distance from the outside perimeter and reaches a maximum in the center. A strong sheath flow keeps the particle stream at the center of the column in the region of maximum supersaturation.

through undetected. Therefore, the CCN chamber reports the number of CCN that activate at a given supersaturation, as shown in Figure 3.6.

3.3.6 Measurements of Ocean Chemistry

In order to resolve the composition of the particles produced from the atomizer (see Section 3.3.2), analytical measurements of seawater composition were conducted on all seawater samples, before and after dialysis. Specifically, the salinity and the concentration of dissolved organic matter (DOM) in the seawater samples were quantified using ion chromatography (IC) and dissolved organic carbon (DOC) analytical techniques.

IC is an analytical technique used to separate and quantify the concentrations of dissolved ions in a sample. The sample is injected into a column containing a fixed resin, and the dissolved ions in the sample bind to the resin in the column. Then, the eluent, an ion exchange solution, flows through the column, and ion species in the eluent compete with and replace the sample ions bound in the column. As the eluent exchanges with the sample ions, they are flushed from the column and measured using a conductivity detector. Ionic affinity to the resin determines the amount of time required for ion exchange by the eluent and varies with each ion. As a result, the dissolved ions in the sample are displaced from the column at different times and detected separately. Based on a calibration with ion standards, the mass concentrations of the ions are determined from the conductivity measurements.

The seawater samples were analyzed on an anion IC system (Dionex ICS-5000) to measure the chloride ion concentration to infer the salinity of the seawater. Salinity is described as a conservative property of seawater, meaning the dissolved inorganic ions are always present in constant proportions to each other (Pilson, 2013). As a result, the salinity of seawater, in parts per thousand (ppt), can be evaluated by multiplying the concentration of the chloride ion (mg L^{-1}), the most abundant dissolved constituent of seawater, by 0.0018066 (Johnson et al., 2007).

A DOC analyzer can measure the concentration of dissolved carbon in a water sample. Before analysis, the sample is acidified and sparged to remove inorganic carbonate compounds. Then, the sample is combusted at a high temperature, causing the sample to be vaporized. During the combustion process, the organic compounds volatilize and form CO_2. The vapor products flow through a dehumidifier and a scrubber to remove water vapor and other unwanted components. Next, the CO_2 passes through an optical detector. Finally, the signal from the detector is compared to a standard calibration curve to report the concentration of dissolved organic carbon in the sample.

Before analysis, the seawater to be analyzed for DOC was acidified using 6 M HCl to stabilize the organic matter in the sample; 25 µL of HCl were added for every 10 mL of seawater. The acidified samples were placed in pre-combusted glass vials (Fisher Scientific, 139-20C) and stored in a refrigerator. All DOC samples were shipped to the University of North Carolina Wilmington where the DOC analysis was performed by Dr. Joan Willey and Paige Powell. Pure water blanks were prepared using Milli-Q water

(Millipore A10) and were included with each shipment of samples to ensure contamination was not present.

As DOM comprises a variety of chemical components other than carbon in the ocean, a correction factor has to be applied to the DOC measurements to account for the total mass of DOM. Previous modelling studies have used an OM/OC ratio of 1.4 for organic compounds in primary SSA (Tsigaridis, 2013). The OM/OC of 1.4 in primary SSA emissions is less than 1.8, the OM/OC representative for typical organic aerosol in the atmosphere (Zhang, 2005), because the primary organics have not undergone oxidative aging. As such, DOC measurements in this study are corrected by a factor of 1.4 to convert to DOM.

3.4 Inferring κ from Measurements

Using the suite of instruments that were previously described, the hygroscopicity parameter, κ, of the generated particles can be inferred from the measurements. In the discussion of κ-Köhler theory, equations 1.5 and 1.6 (Section 1.3) identified that only two variables are required to infer κ for aerosols of unknown composition: critical supersaturation (S_c) and dry particle diameter (D_d). Since the DMA and CCN chamber permit both S_c and D_d to be controlled during measurements, we determined κ using the S_c and D_d.

As particle diameter has a direct influence on CCN activation, particles of the same composition will exhibit different activation behavior at different sizes. By holding the
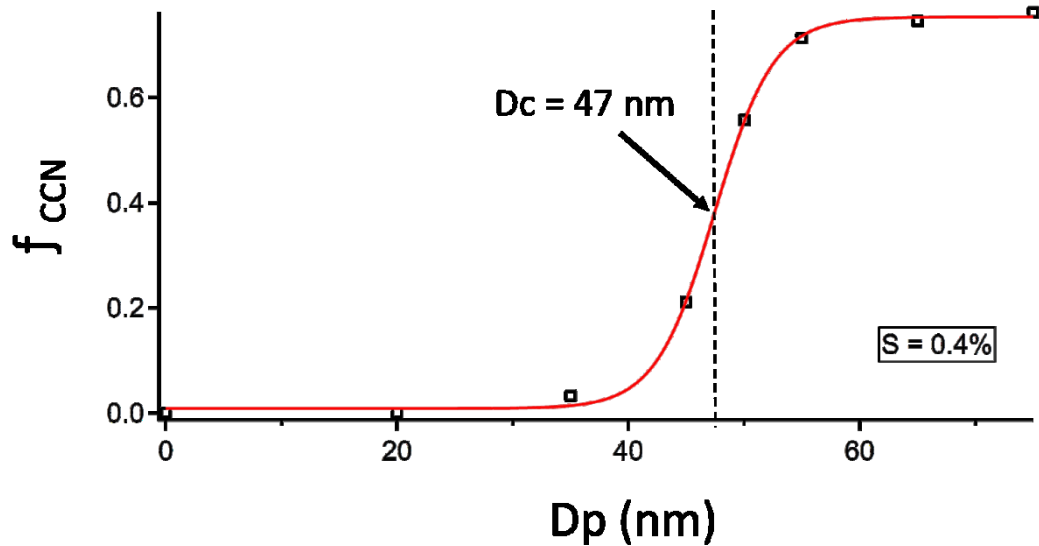
Figure 3.7   An example activation curve for ammonium sulfate to show the determination of the critical diameter. The black squares are the activated fraction (f_{ccn}) expressed as a function of particle diameter (D_p) in nm. The red line is a sigmoidal curve fit to the data. The critical diameter (D_c), located at the point of inflection on the curve, is identified. It is important to note that the activated fraction never reaches unity due to particle losses in the system; however, the plateau observed at the larger diameters is regarded as 100% activation.

superstation in the CCN chamber constant and manipulating the particle diameter using the DMA, information on the CCN activity as a function of particle diameter for a specified supersaturation is obtained. For each particle diameter, the CPC measures the concentration of particles (# cm^{-3}) that enter the cloud chamber, and the OPC reports the cloud droplet number concentration (# cm^{-3}) that result from these particles. Using these measurements, the fraction of particles that activate as CCN can be determined for each selected diameter. Graphical representation of the activated fraction as a function of particle diameter yields a curve of activation with a characteristic sigmoidal shape (Figure 3.7). From an activation curve, the point at which 50% of the particles activate (determined by the point of inflection on the curve), is called the critical diameter, D_c, and

defines the activation diameter from which κ can be calculated (Petters and Kreidenweis, 2007).

3.5 Determining the Hygroscopicity of Organic Compounds

From equation 1.7 (Section 1.3), the κ value of a mixed-composition particle can be explained by the hygroscopicity of each component. This study simplifies the composition of the aerosol generated from seawater samples by categorizing all seawater components into two categories: organic and inorganic material. By modifying equation 1.7, the total κ (κ_{tot}) inferred from the measurements under the assumption of a binary composition system in the particles is given as:

$$\kappa_{tot} = \varepsilon_{inorg}\kappa_{inorg} + \varepsilon_{org}\kappa_{org} \tag{3.1}$$

where ε and κ represent volume fraction and hygroscopicity, respectively.

In the case where the inorganic salts are completely removed from the seawater sample during dialysis, direct measurements of κ_{org} would be possible; however, as complete inorganic removal is not achieved (see Section 4.3.1 and Appendix A), analytical measurements of seawater chemical composition were utilized in calculations. Since an atomizer was used for particle production, we can assume that the volume fractions of organic and inorganic components are reflective of their concentration in the sample. Likewise, the organic and inorganic concentrations were quantified in each sample using DOC and salinity measurements. As a result, the volume fractions in the particles can be

45

determined. The volume fraction of the organic component in atomized particles (Vf_{org}) was calculated using the following relationship:

$$Vf_{org} = \frac{1}{1 + \frac{mf_{inorg} \, \rho_{org}}{\rho_{inorg} \, mf_{org}}} \qquad (3.2)$$

where mf is the mass fraction of organic and inorganic components in the atomizer solution, and ρ is the density of the organic and inorganic components. The density of NaCl was used for the inorganic compounds as NaCl is the dominant component of seawater, comprising 86% of inorganic mass (Pilson, 2013). The density of the organic component was assumed to be 1.2 g cm^{-3}, a common assumption in the literature for organics in aerosol (Turpin and Lim, 2001). Furthermore, the hygroscopicity of the inorganic salts was identified in the sample. While it has been shown that inorganic ions other than NaCl have a quantifiable impact on the hygroscopicity of sea spray (King et al., 2012), κ_{inorg} for this analysis is assumed to be equivalent to that of NaCl. The same assumption has been applied in previous modelling studies of SSA hygroscopicity (Westervelt et al., 2012). Therefore, using hygroscopicity and seawater chemistry measurements, κ_{tot}, ε_{inorg}, κ_{inorg}, and ε_{org} are known, and the κ of the organic components can be determined.

Analyses were carried out on SML and bulk water samples before and after they were dialysed. As a result, two calculations of κ_{org} can be made from a single sample. After dialysis, κ_{tot}, ε_{inorg}, and ε_{org} measured in the sample are expected to change; however, κ_{inorg} and κ_{org} are anticipated to remain the same, allowing for κ_{org} to be verified by measurements before and after dialysis. Likewise, the analysis permits comparisons of

hygroscopicity measurements to be made between the SML and bulk water. Furthermore, the enhancement of marine organics relative to sea salt from the dialysed samples allows for further insight on the influence of organic composition in reducing the hygroscopicity in the particles.

CHAPTER 4   RESULTS AND DISCUSSION

4.1 Instrumental Uncertainties

In the following experiments, measurement uncertainties were considered for instrumental error in the particle sizes selected by the electrostatic classifier and the supersaturation in the cloud chamber. TSI reports 3% measurement uncertainty in the mobility diameter of particles selected by the DMA used in the present work. The supersaturation uncertainty in the cloud chamber measurements (0.02%) was determined using the standard deviation of a record of calibration data. Using these two instrumental uncertainties, the uncertainty of κ inferred from activation diameters was propagated in quadrature, resulting in a total uncertainty of 12%. This uncertainty is similar to the 10% measurement uncertainty reported in other studies using the same method with this model of CCN chamber (Rose et al., 2008; Dawson et al., 2016). As such, κ measurements within 12% of expected values will be regarded as equivalent in the discussion of the results.

4.2 Control Experiments

Before using the dialysis method on seawater samples, a series of control experiments were designed for prepared solutions to verify the efficacy of the method and to validate key assumptions. The control experiments were performed on solutions of known composition, where each solution was prepared to test a different aspect of the dialysis method. Specifically, tests were conducted to confirm hygroscopicity predictions of mixed organic/inorganic component particles using equation 3.1 (Section 3.5) derived by

κ-Köhler theory and to validate the assumption that the volume fraction of a component in the particles reflects the mass fraction of the component in the sample solution, corrected for density, when generated from an atomizer. Further tests were performed to ensure that the dialysis method does not influence the hygroscopicity of the particles by contaminating the solutions and to demonstrate that the dialysis method can desalt a solution. The results of each control experiment are discussed in detail below.

4.2.1 Hygroscopicity of Mixed Component Particles

As the volume fraction mixing rule defined by κ-Köhler theory (Section 1.3) is critical for quantifying the hygroscopicity of mixed component particles, it is necessary to verify the predicted hygroscopicity of simple organic/inorganic mixtures to conduct similar analyses on seawater samples. In addition, the assumed volume fraction of organic/inorganic components in particles generated from an atomizer is a key assumption to these analyses, as it allows for the volume fraction of the particles generated from seawater samples to be quantified by measurements of salinity and DOC. For these tests, solutions were prepared by dissolving known quantities of mannitol and NaCl, used as model organic and inorganic compounds, in deionized water. Multiple solutions were prepared with varying mass ratios of dissolved NaCl and mannitol, and particles were generated from the solutions using an atomizer. The volume fractions of mannitol and NaCl in the particles were calculated using the mass ratio of the components in the solutions, as discussed in detail in section 3.4. Prior to analyses of the mixed solutions, the hygroscopicity of NaCl and mannitol were measured individually from pure, single-component solutions. κ_{inf} was
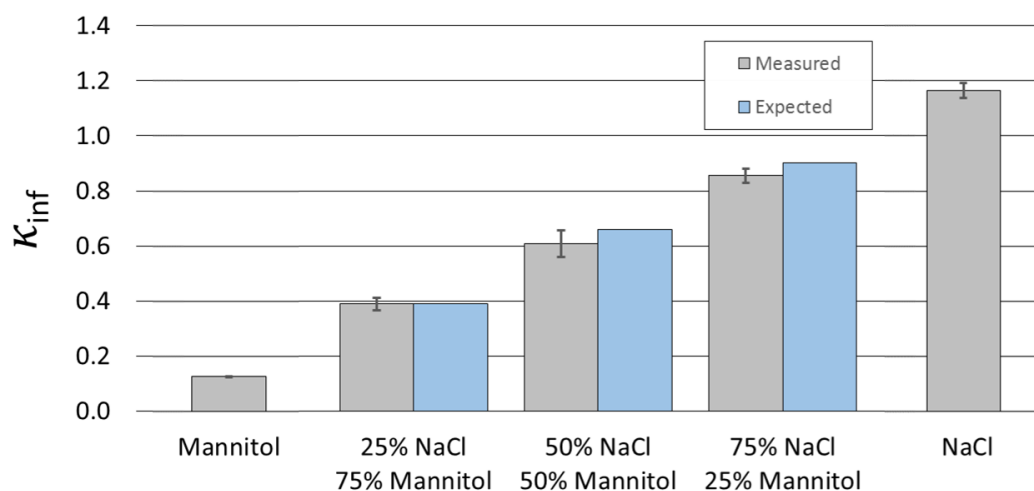
Figure 4.1   Measured and expected κ_{inf} for particles with mixed organic/inorganic composition.

measured to be 1.17 and 0.13 for NaCl and mannitol, respectively. Using the measured κ

for the individual component particles and the assumed volume fraction of mannitol and

NaCl in the mixed component particles, the total κ was predicted for particles generated

from each of the mixed solutions.

Comparisons between the measured and expected κ from the mixed component particles

are summarized in figure 4.1. The hygroscopicity of particles generated from the mixed

solutions, containing three variable mass ratios of NaCl and mannitol, show excellent

agreement between measurements and theoretical predictions. Deviations of κ_{inf} from the

expected values range between 0.5 – 8%, which is within measurement uncertainties. This

agreement confirms κ predictions for simple mixed organic/inorganic aerosol using the

volume fraction mixing relationship and validates the assumption that the particle

composition does not deviate from the composition of the sample solution in the atomizer.

4.2.2 Influence of Dialysis on Hygroscopicity

The next set of control experiments were used to test for contamination of samples during the dialysis process. To prevent microbial growth in the dialysis membrane during storage, the membrane is kept in a sodium azide preservative solution in a refrigerator. Prior to use, the membrane is rinsed and soaked in deionized water to remove the preservative. Furthermore, the dialysis membrane itself is composed of a cellulose material which is subject to degradation under certain conditions. If any of these precautionary measures fail, contamination in the dialyzed solution would result in compositional changes that could influence the hygroscopicity of the generated particles. Additionally, if the preservative is not removed or the membrane loses its integrity and breaks down in the sample, the composition of the solution could be contaminated.

Several single-component stock solutions containing NaCl, mannitol, and bovine serum albumin (BSA, a beef protein) were prepared and then dialyzed using the method described in Section 3.3; however, instead of using deionized water as the dialysate solution, each solution was dialyzed in a dialysate with the same composition of the dialyzing sample. This modification to the method was used to ensure that the dissolved components were not completely removed during the dialysis process. After dialysis, each solution was atomized and the hygroscopicity of the particles were measured. Figure 4.2 summarizes the hygroscopicity of the particles generated from the solutions before and after dialysis. The measurements before and after dialysis show $2 - 12\%$ change for the three solutions. Such a result implies that there is no significant source of contamination

from bacterial growth, excess preservative, or membrane degradation during the dialysis process.

Further tests for contamination were carried out with deionized water to characterize the influence of residual compounds that remain in the atomizer between sample runs. The deionized water was flushed through the atomizer, atomized, and the resulting particle size distributions were measured. The number of particles produced from the water were found to be negligible compared to the number concentrations generated from the samples. Such a result indicates that cross contamination between samples is insignificant, and the atomizer cleaning procedure is effective.
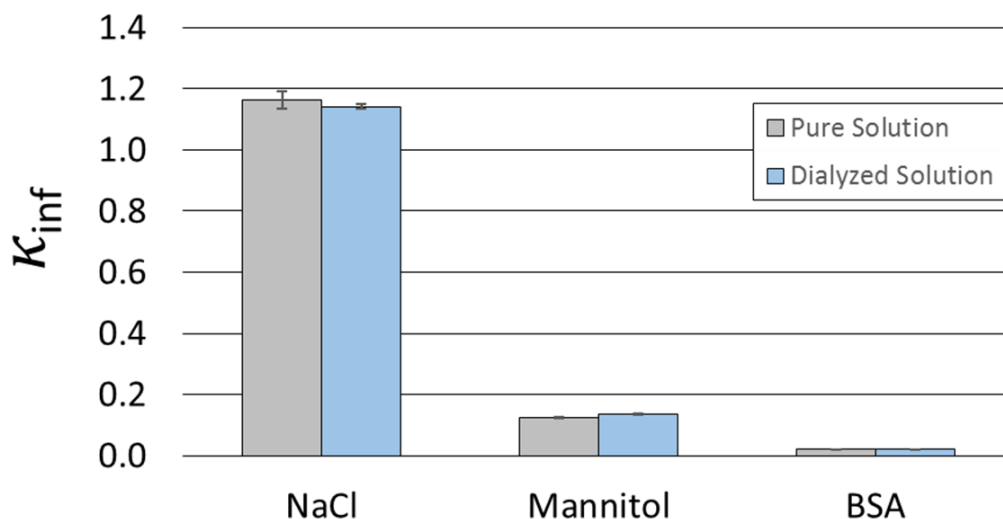
Figure 4.2   Comparison of hygroscopicity measurements for single-component stock solutions before and after dialysis.

4.2.3 Dialysis with Control Solutions

An additional experiment was performed to illustrate the concept of desalting a sample and isolating an organic component. The tests aimed to achieve complete removal of the inorganic components using dialysis while retaining the organic compounds. BSA was selected for use in this test because it is a large compound with a molecular weight of ~ 66,000 g mol^{-1}. The large size of BSA is advantageous for this experiment, because it ensures the retention of BSA during dialysis. For this test, a solution of 40% BSA and 60% NaCl by mass was prepared and dialyzed. The hygroscopicities of the particles from the atomized solutions were evaluated before and after dialysis and compared to the expected values, as summarized in Figure 4.3. Before dialysis, the expected κ_{inf} was predicted using κ-Köhler theory for the solution of BSA and NaCl; after dialysis, κ_{inf} is expected to be the same as κ_{inf} measured for pure BSA particles.
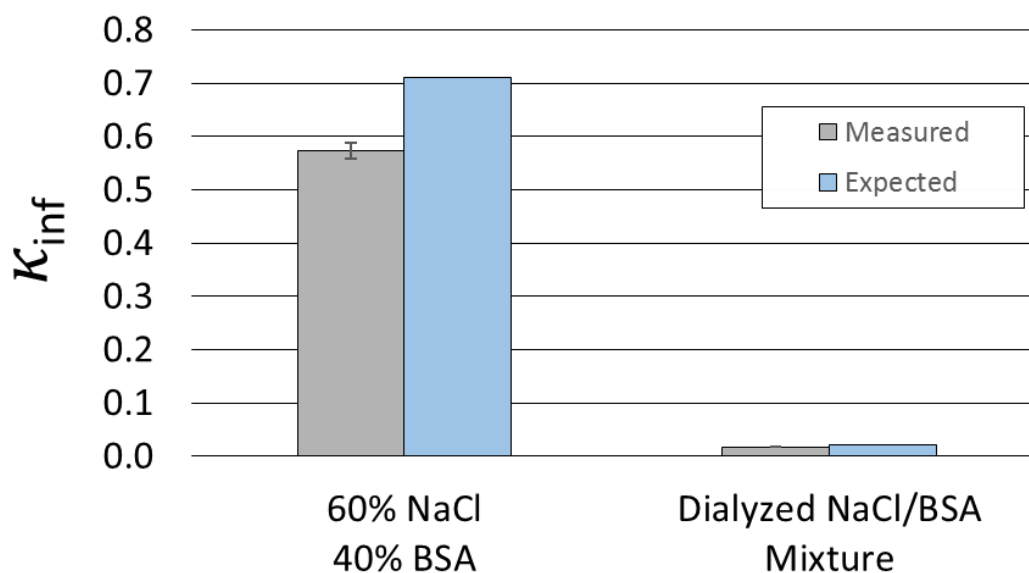
Figure 4.3   Measured and expected κ_{inf} of an organic/inorganic mixture before and after dialysis.

Even though the κ_{inf} for the BSA/NaCl mixture before dialysis shows a greater difference between the measured and expected values (19%) than the instrumental uncertainty, κ_{inf} is significantly reduced in the solution after two weeks of dialysis. The reduction in hygroscopicity measured for the dialyzed BSA/NaCl solution ($\kappa_{inf} = 0.017$) demonstrates that NaCl was removed from the sample and the hygroscopicity of pure BSA particles was recovered ($\kappa_{inf} = 0.02$). One possible explanation for larger deviations between the measured and expected values in this experiment could be due to partial denaturing of BSA in the samples. Specifically, different concentrations of NaCl can influence the stability of BSA in a solution (Giancola et al., 1997). As a result, structural changes of BSA in the solution are possible and may also occur during atomization. Such changes in the structure of BSA may have an influence on the hygroscopic properties of the resulting particles, however, this hypothesis was not tested further in the context of this experiment. Despite these differences, the results of this test prove the effectiveness of using the dialysis method and serves as an ideal scenario for processing seawater samples.

4.3 Analyses of Seawater Samples

Concurrent SML and bulk water samples were collected from the Northwest Arm in Halifax, Nova Scotia during September 2015, November 2015, and January 2016. Each of the samples was processed using the dialysis method (section 3.3) and atomized to infer the hygroscopicity of the generated particles (section 3.7). For each sample, the hygroscopic properties were compared before and after dialysis, and measurements of

seawater chemistry were used to evaluate the contribution of the organic and inorganic

components according to the volume fraction mixing relationship (equation 3.1, section

3.8). The results of the analyses are discussed below.

4.3.1 Effectiveness of Dialysis

During the development of the method, dialysis proved to be an effective desalting

mechanism when used for artificial and filtered seawater solutions by reducing the salt

concentration in a sample from 35 g L^{-1} to ~10 mg L^{-1} (see Appendix A). In addition, a

control experiment demonstrated the ability of organic isolation from a mixed component

solution via dialysis, as previously discussed. Dialysis on real seawater samples, however,

was not as effective as the control scenarios. The total inorganic ion concentration in the

seawater samples before dialysis ranged from 26 – 35 g L^{-1}. After dialysis, sea salt

concentrations were reduced to 280 – 620 mg L^{-1}, an order of magnitude higher than the

reduction in the dialysis tests. Replicating the results of the control situation, where the

organic component was completely isolated, was unattainable using real seawater. While

the cause for the higher concentrations of inorganic components after dialysis in the

seawater samples is unknown, one possible explanation could be that larger organic

molecules from the real seawater samples clog the pores in the dialysis membrane and

block the diffusion of salts from the sample. Regardless, the concentrations of organic and

inorganic components are measured in the seawater samples before and after dialysis,

allowing the influence of both components on particle hygroscopicity to be quantified in

unprocessed seawater as well as seawater with an enhanced organic composition.

4.3.2 Hygroscopicity Measurements
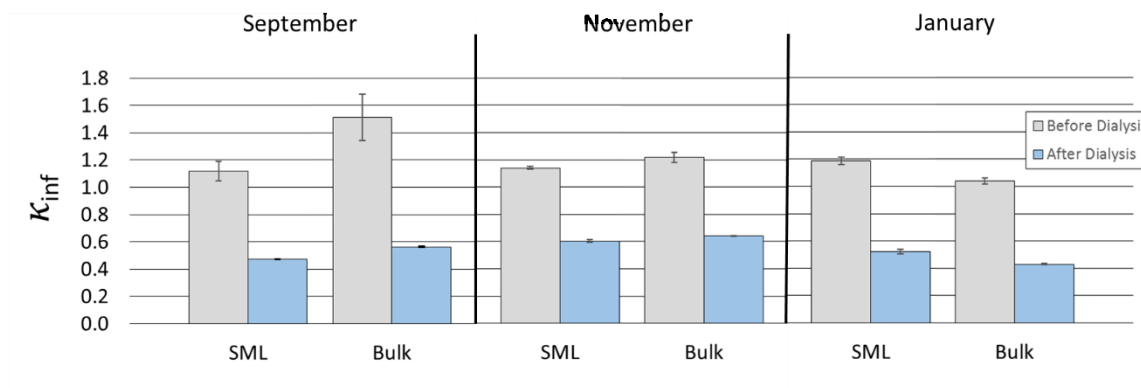
Figure 4.4   Inferred hygroscopicity measurements of SML and bulk water samples
before and after dialysis.

A comparison of the hygroscopic measurements taken for the SML and bulk water

samples before and after dialysis for all months sampled are summarized in Figure 4.4.

Upon initial assessment, the results presented in Figure 4.4 are as expected. For each of

the undialyzed seawater samples, including both SML and bulk water, κ_{inf} ranges from

1.04 – 1.51 with an average of 1.20. The average hygroscopicity for the raw seawater

samples is in excellent agreement with our measurement of NaCl particles ($\kappa_{inf} = 1.17$),

and agrees with the literature values for pure NaCl ($\kappa_{NaCl} = 1.28$) (Petters and

Kreidenweiss, 2007) within the instrumental uncertainties. In addition, the measurements

of κ_{inf} for natural seawater in the present work occur within the ranges reported from other

studies (Neidermeier et al., 2008; Collins et al., 2013; Schill et al., 2015). These observed

hygroscopicities suggest that the composition of the atomized particles from the raw

seawater samples is dominated by sea salt in the SML and bulk water, and there is no

observable difference between the SML and bulk water samples. The range of κ_{inf}

measured from the samples before dialysis could be explained by variation in the

composition of inorganics in the particles. A study by King et al. (2012) found that the hygroscopicity of particles generated from artificial seawater deviates from that of pure NaCl; they suggest that interactions between inorganic ions in the particles result in different particle morphologies that can influence hygroscopicity (King et al, 2012).

In addition to the agreement among the raw seawater samples, Figure 4.4 illustrates the observed differences in κ_{inf} between samples before and after dialysis. In each sample, there is a significant reduction in κ_{inf}, ranging from $47 - 62\%$, after the sample is dialyzed. Since the dialyzed samples have a reduced concentration of inorganic salts, which are expected to be more hygroscopic than the organic components, the reduction in hygroscopicity is in line with our expectations. Likewise, the degree of hygroscopic reduction is similar for SML and bulk water samples and remains comparable between the three months sampled. Such a result illustrates consistency and reproducibility in the sample processing methods and hygroscopicity measurements.

4.3.3 Analytical Measurements of Seawater Composition

Analytical measurements of salinity and total organic carbon were utilized for determining the volume fraction of the inorganic salts and organic compounds in the atomized particles. A summary of the seawater chemistry measurements for all samples is included in Table A.1 in Appendix A. Unsurprisingly, inorganic salts were found to dominate in the seawater samples. Before dialysis, the mass fraction of the inorganic components was measured to be 99.99% in all SML and bulk water samples. The high mass fractions of

inorganics confirm that sea salt dominates the hygroscopic properties and the organic component is negligible for the seawater samples before dialysis.

Despite reduced inorganic concentrations, sea salt was also found to dominate in the dialyzed samples. After dialysis, the inorganic mass fractions in the samples ranged from 98 – 99.6%. Therefore, the dialyzed samples only have a 0.4 – 2% enhancement of the organic component relative to the raw seawater. Given the significant reduction in particle hygroscopicities measured between dialyzed and undialyzed samples, the high mass fraction of the inorganic compounds is unexpected in the dialyzed samples.

4.4 Evaluating Measurements with Theory

The seawater chemical analyses were used to calculate the expected κ using equation 3.1 and compared to the observed hygroscopicities. In each collected seawater sample, for the SML and bulk water, the significant reduction in hygroscopicity observed for the dialyzed samples does not agree with κ-Köhler theoretical predictions.

To illustrate the discrepancy between the measurements and theoretical predictions, the data for the September SML sample before and after dialysis (summarized in Figure 4.5) are discussed in further detail. κ_{inf} for the September SML sample was measured to be 1.12 and 0.47 before and after dialysis, respectively. As the inorganic component comprises 99.99% of the dissolved mass in the undialyzed sample, we can assume the mass fraction of the organic component is negligible; thus, $\kappa_{inf} = \kappa_{inorg}$. After dialysis, the mass fraction of the inorganic ions is reduced to 98.9%. The high persistence of inorganics
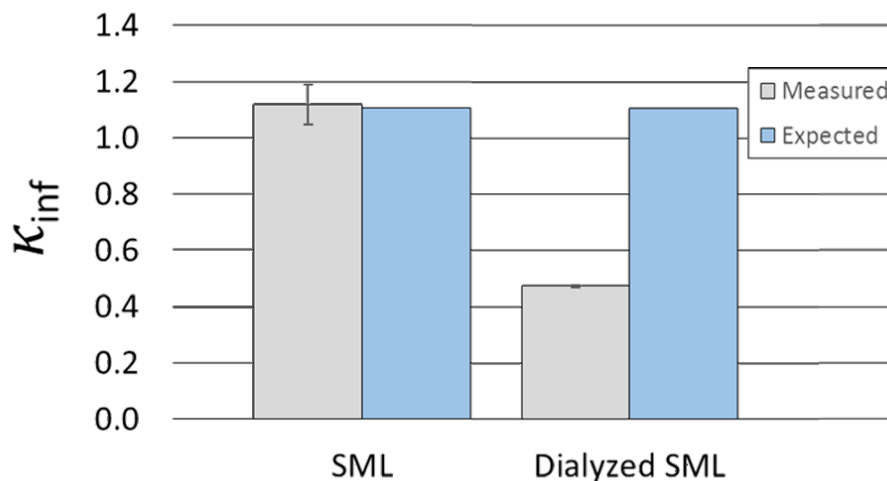
Figure 4.5   Summary of measured and expected values for the September SML samples before and after dialysis. The expected values are calculated based on the chemical composition of the seawater samples.

in the sample after dialysis suggests that the reduction in hygroscopicity would be less than was observed. For example, assuming the organic components are completely non-hygroscopic ($\kappa_{org} = 0$), theory predicts that 98.9% of dissolved inorganic mass in the solution results in $\kappa_{inf} = 1.11$, which is 136% higher than the observations ($\kappa_{inf} = 0.47$) and differs from κ_{inorg} by less than 1%. An additional way of highlighting the discrepancy after dialysis is to consider the observed and predicted ε_{inorg} in the particles using the hygroscopicity measurements. By again assuming $\kappa_{org} = 0$ and $\kappa_{inorg} = 1.12$, theory predicts ε_{inorg} in the particles to be approximately 42%, which is significantly lower than the measured volume fraction ($\varepsilon_{inorg} = 98.9\%$).

The inconsistency of measurements and theory for the September SML sample is not unique; a significant difference between the measured and expected hygroscopicities was
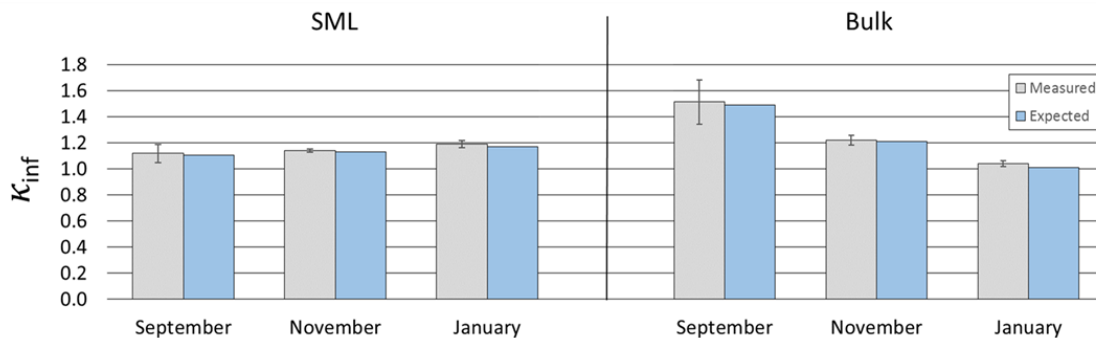
Figure 4.6   Measured and expected κ_{inf} for raw seawater samples.
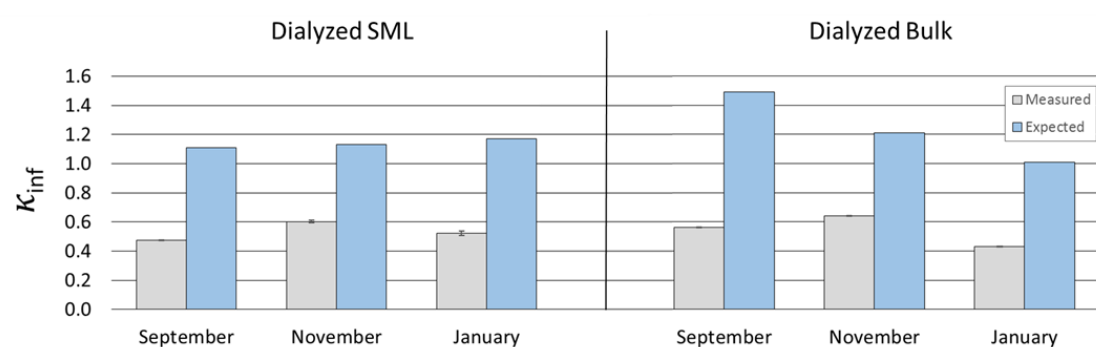
Figure 4.7   Measured and expected κ_{inf} for dialyzed samples.

observed for each dialyzed seawater sample. Applying the same assumptions for theoretical predictions as discussed for the September SML sample, Figures 4.6 and 4.7 depict a comparison of the measured and expected κ_{inf} for all analyzed samples before and after dialysis.

Figure 4.7 illustrates that we observe a significant difference between the measured and expected hygroscopicities of particles generated from seawater with only slightly reduced inorganic concentrations. While the mechanism remains inconclusive, the divergence between the measurements and theory suggests that the organic composition in seawater has a more significant influence on the hygroscopic properties of SSA than previously

thought. Such a result is in opposition to previous studies, which observe that hygroscopic salts dominate the CCN activity in SSA enriched with biogenic organics (King et al., 2012; Fuentes, et al., 2011; Wex et al., 2010). These studies, however, take a different approach to their measurements than the work presented in this thesis. While each study examines the effect of biological organic material on the hygroscopic properties of SSA, the researchers used artificial and filtered seawater solutions that were spiked with a known amount of organics, typically algal exudates. A similar approach was used in this thesis and showed that these methods follow the expected results (Section 4.2.1). In addition, Fuentes et al. (2011) focused their measurements on organic matter < 0.2 μm by filtering the samples before analysis. Therefore, the raw, unfiltered seawater samples analyzed during this work are likely to contain a more complex matrix of organic compounds as well as larger compounds than previous studies, which may in part explain the different results presented herein.

4.5 Discussion

4.5.1 Contamination from Dialysis

The unexpected results could be due to a systematic error in the method that generates a bias in the hygroscopicity measurements. One possible source of systematic error could include contamination of the sample during dialysis. As the deviations from theory occur in the samples after dialysis, it is reasonable to infer that the problems may occur during the dialysis process; however, there is experimental evidence demonstrating that dialysis does not contaminate the samples. In addition to the success of the control experiments testing for contamination from the dialysis tubing, as previously discussed, the

measurements of organic carbon in the seawater before and after dialysis do not indicate a significant source of contamination in the sample during processing. A summary of the chemical composition of the seawater samples is provided in Table A.1 in Appendix A. We expected a small amount of low molecular weight dissolved organic compounds to be lost during dialysis, and such a reduction was evidenced by a lower concentration of organic carbon measured for each of the SML samples after dialysis. Unexpectedly, for each bulk water sample, the measurements show that there was an increase in the organic carbon concentrations after dialysis. The increase was only observed in the bulk water samples, and establishes that further characterization of organic carbon in the seawater is necessary for the analysis of future samples. While higher organic carbon concentrations after dialysis could signify contamination, the increase is not large enough to resolve the discrepancies in hygroscopicity between measurements and theory for the samples before and after dialysis.

4.5.2 Composition during Atomization

Another source of systematic error could result during particle generation from the atomizer. The relationship between the composition of the solution and the composition of the particles generated during atomization, as discussed in Section 3.3.2, is a fundamental assumption of the present work. Other studies of mixed-component particle properties make use of the same assumption (Prisle et al., 2010; Dawson et al., 2016); however, the production of externally mixed particle populations have been observed in atomized solutions containing insoluble components (Creamean et al., 2014). In addition, Petters and Petters (2016) report unexplained scatter measurements during atomization

experiments using an organic control molecule which they explain by suggesting that low-solubility and surface active organic compounds in a solution can change during atomization, leading to particle compositions that deviate from stock solutions. Furthermore, a study comparing the effects of different particle generation mechanisms reports that large organic components may break apart during atomization (Fuentes, 2010). The results of the previous studies indicate that particle composition produced from the atomizer may not reflect the composition of the solution in the seawater samples, as it is possible the samples contain insoluble components, particulate organics, and surface active organics. Further characterization of the influence of particulates on the hygroscopicity of the samples by comparing filtered and unfiltered seawater is necessary to address these possibilities.

To address the possibility that the chemical composition of the atomized particles were not reflective of the solution, a series of experiments were attempted to verify the assumption of particle composition from the atomizer. Three different approaches were employed: filter measurements, fluorescence microscopy, and mass spectrometry of the particles. While the mechanism of identifying the particle composition in each approaches differ, all methods aim to provide a quantitative measure of the volume fraction of organic and inorganic components in the particles to assess the validity of our assumptions. For the filter method and the mass spectrometer measurements, the mass of the components can be quantified using analytical techniques. The fluorescence microscopy technique uses visual inspection of particle aggregations, where fluorescence allows for organic components to be identified separately from the inorganics compounds. Each method has different advantages and disadvantages to their analyses. Tests have been conducted for

each approach, however, conclusive results have yet to be achieved with any of the methods. Further details on the techniques and the experimental work completed using the different methods are included in Appendix C. In the future, additional tests using these methods are required to provide closure to the composition of the seawater particles generated from the atomizer.

Despite the possibility of several types of particle compositions produced from the atomizer, the activation curves provide evidence of a uniform composition in the particles generated from the atomized seawater samples. Schill et al. (2015) show that activation curves of externally mixed aerosol can capture the hygroscopicities of the different particle compositions when using high resolution scans of superstation. By comparing activation curves of pure component particles and externally mixed aerosol under controlled conditions (Figure 4.8), they found that high resolution scans can resolve the activation diameters of the individual components. Without the use of high resolution scans, they observed that activation curves in externally mixed aerosol exhibit a shallower increase in the fraction of activated CCN (Schill et al., 2015). Figure 4.9 depicts activation curves of supersaturation scans for atomized seawater particles. Given the steep increase in f_{CCN} in our activation curves, it is reasonable to infer that particle composition is uniform during atomization.
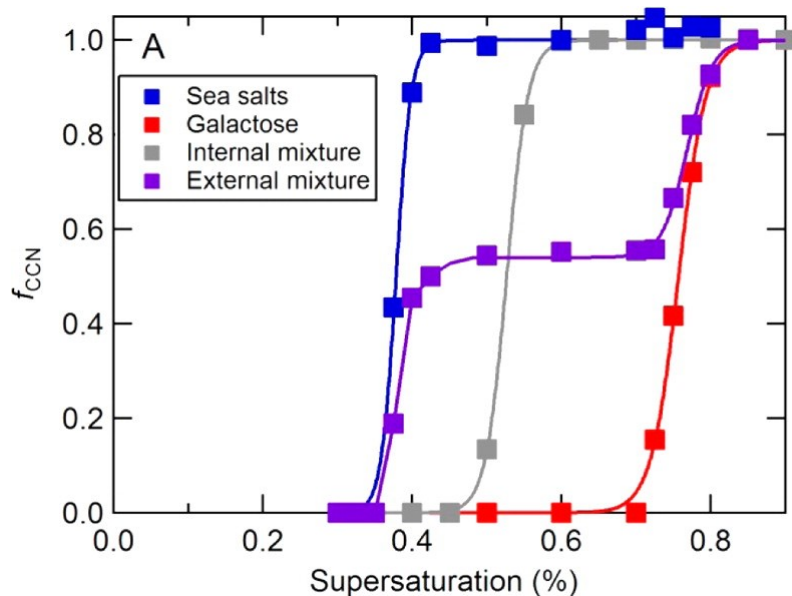
Figure 4.8   Activations scans of externally and internally mixed aerosol. Adapted from (Schill et al., 2015).
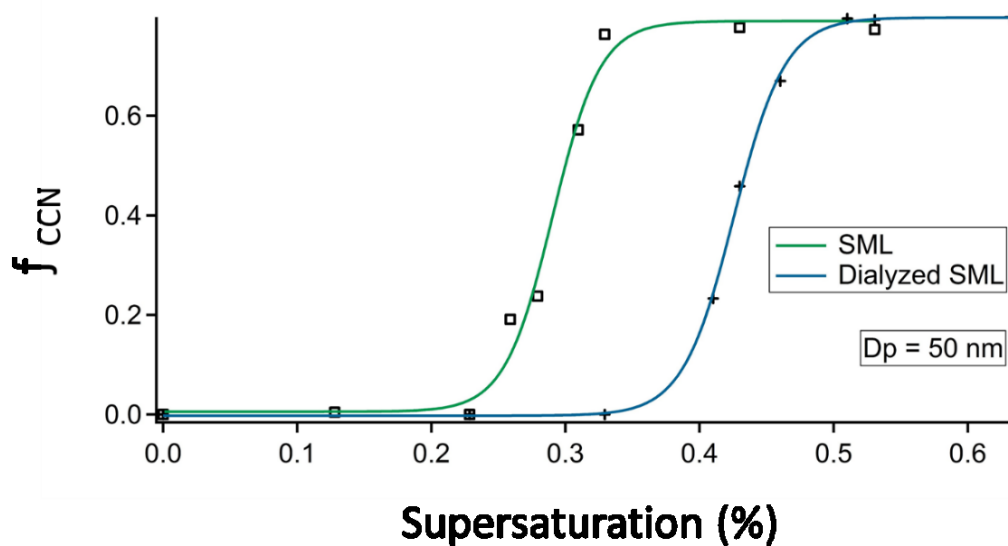

Figure 4.9   Activation curves for supersaturation scans of seawater samples. The curves show CCN activation for the November SML sample before and after dialysis. The steep increase in f_{CCN} implies internally mixed particles of uniform composition. Both curves were corrected for the influence of double-charged particles.

4.5.3 Phase Separation

Another possible explanation for the differences in our observations could include phase limited cloud droplet activation behavior. It has previously been found that atmospheric aerosol particles or mixed organic/inorganic composition exhibit liquid-liquid phase separation, where aqueous organic and inorganic compounds in a particle will separate based on differences in miscibility (Marcolli and Krieger, 2006; Ciobanu et al., 2009; You et al., 2012). Petters et al. (2006) suggested that the miscibility limitations of organic compounds in aqueous aerosol can result in CCN activation behavior that deviates from traditional Köhler theoretical predictions. Further observations have identified that phase separation in particles has an influence on hygroscopic growth factors derived under sub-saturated conditions, causing differences between measurements and theoretical predictions (Hodas et al., 2015). Likewise, studies have modelled the CCN behavior in phase-separated organic particles and found that the presence of two phases near 100% relative humidity can affect droplet activation by elevating the saturation required for droplet activation (Figure 4.10) (Renbaum-Wolff et al., 2016; Petters et al., 2016). These models are similar to the model proposed by Bilde and Sveningsson (2004), which explains the possibility of similar behavior for particles where solubility limitations exist.

The presence of phase separation in our seawater samples was briefly explored to test if phase separation could explain our unexpected results. As the hygroscopicities that we inferred after dialysis were much lower than expected and our samples are expected to contain surface active organics, the effect of miscibility limitations on CCN activation, as shown in Figure 4.10, seemed to be a possible explanation for our results. However,
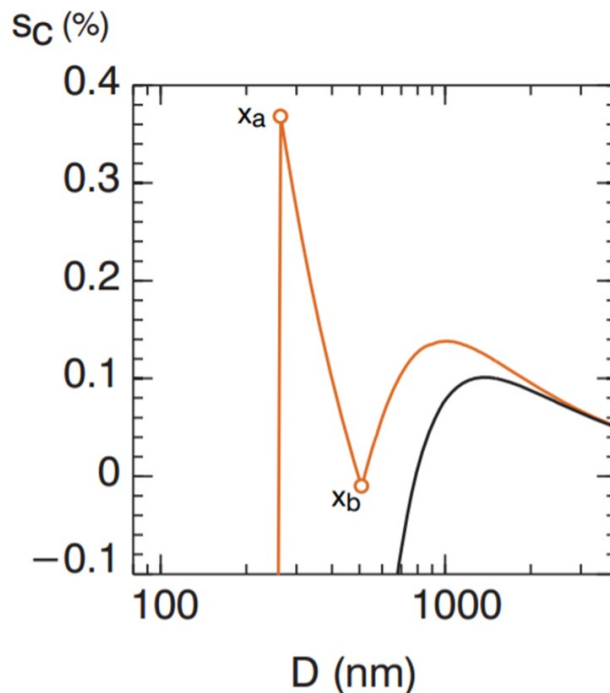
Figure 4.10   Modelled Köhler curves for phase separated organic aerosol. The black line shows a traditional Köhler curve without phase separation, and the orange line depicts the activation behavior of a phase separate particle. D represents the wet diameter of a growing droplet. The hollow circles indicate the mole fractions (X_a and X_b) within which phase separation is expected to occur within the aqueous droplet. The initial increase in S_c as a result of phase separation is higher than the supersaturation for CCN activation predicted by Köhler theory. As such, the first peak determines the supersaturation that must be achieved for the particle to activate. Adapted from (Petters et al., 2016).

calculations of a model particle prove that phase separation does not give a feasible justification. The low volume fraction of organics in the particles (<3%) can only provide an organic coating 3 angstroms thick for a dry particle diameter of 50 nm. As the particle takes up water and swells, the low volume of organics would be inadequate to cover the aqueous phase droplet. Furthermore, observations of particle composition using fluorescence microscopy, as described in Appendix C, shows that the dissolved inorganic/organic constituents in an aqueous droplet from a bubbled seawater solution are
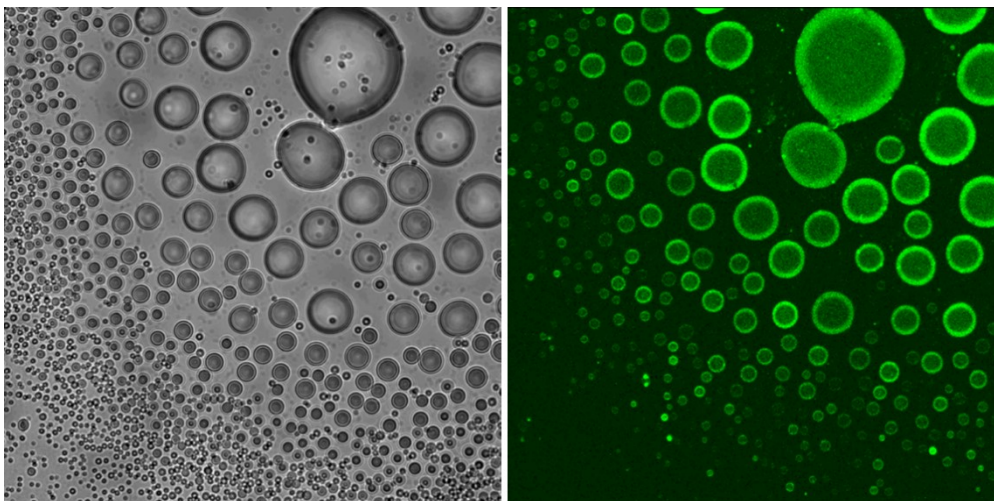
Figure 4.11 Fluorescence microscopy images for bubble seawater water particles at high relative humidity (close to 100%). The volume fraction of organic component in the particles is ~40%. The uniform fluorescence through the center of the droplet indicates that the organic and inorganic compounds are well mixed in the liquid phase. The ring around the edges of the droplets are due to a lensing effect and can be ignored. Figure by Dr. James Grayson from University of British Columbia.

well mixed (Figure 4.11). Therefore, it is highly unlikely that phase separation effects contribute to our observations.

4.5.4 Droplet Growth Kinetics

Limitations on droplet growth kinetics due to particle composition effects may also be relevant in our particles. During the CCN measurements, it is assumed that the droplets are in equilibrium with respect to water vapor, but it is possible that the composition of the particle makes this assumption false. Currently, there is a lack of consensus on the subject of droplet activation kinetics. Several studies have identified that the kinetics of water uptake may be important for CCN concentration in aerosol with high prevalence of organic composition (Murphy et al., 2009; Shantz et al., 2010; Ruehl et al., 2008), while

others show that particle composition has no influence on droplet growth (Bougiatioti et al., 2011; Cerully et al., 2011; Padro et al., 2012). Furthermore, droplet growth kinetics in the subsaturated regime for sea salt particles enriched with algal exudates were found to be inconsequential on the order of 3 – 10 seconds, suggesting the organics do not affect droplet kinetics (Wex et al., 2010). As the organic composition of the seawater particles are measured to be < 2% of the total volume fraction, droplet growth kinetics are not expected to have an effect on our samples; however, further exploration of droplet growth kinetics in the generated seawater particles could provide useful insight. The influence of particle composition on droplet growth kinetics is typically characterized by comparing the cloud droplet size distributions of samples and calibration aerosol (e.g. Murphy et al., 2009; Engelhart et al., 2008; Zhao et al., 2016; Shantz et al., 2010). The droplet growth distributions, which are measured by the CCN chamber used in our experiments, could be further analyzed using these methods to probe for kinetic effects.

4.5.5 Marine Microgel Formation

An additional aspect of our sample analyses that may have important ramifications on our results include the formation of marine microgels in seawater. Marine microgels, or hydrogels, are globular assemblages of dissolved organic material that form as a result of cross-linking between polymer chains (Verdugo, 2004). The formation of these colloidal aggregations of dissolved organic matter can occur on the timescale of minutes, and their properties are sensitive to environmental conditions such as temperature, pH, and ionic concentration (Tanaka, 1992). Further analysis of microgel formation demonstrates that the biopolymer aggregations are ionic in nature; the stability of formation depends on the

presence of Ca^{2+}, and microgel formation is disrupted when cations (Ca^{2+} and Mg^{2+}) are removed from solution (Orellana et al., 2011). Microgel formation has been found to occur within the organic composition of the SML (Cunliffe et al., 2013), and marine microgels have been observed in clouds and fog in the Arctic (Orellana et al., 2011).

These previous studies suggest that marine microgels are likely present in the collected bulk and SML samples. Furthermore, due to the sensitivity of microgel formation on the availability of inorganic ions, the process of dialyzing the samples is likely to directly affect the interactions between the dissolved organic components in seawater. A study by Dawson et al., (2016) made hygroscopicity measurements for control experiments using a biopolymer proxy mixed with inorganic compounds in atomized solutions. They found agreement between their observations and κ-Köhler theory predictions for CCN measurements; however, at subsaturated conditions, significant deviations were observed. They conclude that different salt concentrations could be explored to resolve the differences in the measurements (Dawson et al., 2016). While the results in this thesis oppose the observations of Dawson et al. (2016) for CCN activity, their observations at subsaturated conditions highlight that microgels in particles can influence hygroscopic properties.

Similarly, an additional study by Leck and Svensson (2015) found that the CCN behavior of ambient aerosol in the arctic deviates from κ-Köhler theory. They show that theory over predicts the measured concentrations of CCN by as much as 30 – 60% in some cases. Furthermore, their observations indicate that marine microgels comprise a significant portion of the aerosol in the Aitken mode, and they hypothesize that the differences

between the measured and expected CCN concentrations are due to interactions between

hydrophilic and hydrophobic constituents in aerosols containing microgel that are not

captured by theory (Leck and Svensson, 2015). Further consideration of the concentration

of salt and its influence on microgel formation in the generated aerosol may provide

additional insight to the unexpected results in the present work.

CHAPTER 5   CONCLUSIONS AND FUTURE WORK

5.1 Conclusions

The primary objective of the work conducted in this thesis is to determine the hygroscopicity of organic components in SML and bulk water samples using laboratory measurements. A dialysis method was developed and employed to decrease the concentration of inorganic salts in seawater solutions while the organics are retained. Particles were generated from seawater samples before and after dialysis using an atomizer, and instrumental analyses were used to infer κ for the particles by evaluating CCN activation curves. By combining the hygroscopicity measurements with the measured chemical compositions of the seawater components, the hygroscopic properties of the samples and the organics were evaluated.

Hygroscopicity measurements of all bulk and SML samples before dialysis were found to agree well with the accepted hygroscopicity of NaCl and to fall within the range of natural and artificial seawater measurements from previous studies. These results also agree with measurements of seawater chemistry, where inorganic salts were measured to be 99.99% of particle volume in each raw seawater sample; the influence of organic components on particle hygroscopic properties were found to be negligible.

Using dialysis to desalt the seawater samples proved to be less effective on seawater solutions than for controlled solutions; complete isolation of the organic components was not attainable. Inorganic mass fractions in the seawater samples remained as high (~98%)

after dialysis. Despite the prevalence of inorganic salts, a significant reduction in the hygroscopicity of particles generated from the dialyzed samples was observed. The reduction was seen in every sample, both bulk and SML, for all three months sampled. Comparing the measurements with the volume fraction mixing relationship of κ-Köhler theory, our observations show significant discrepancies (> 50%) from the theoretical predictions. The deviations in the measured and the expected hygroscopicities suggest that κ-Köhler theory fails to capture the mechanism by which small quantities of organics in sea spray and ocean organics have a more significant influence on the hygroscopic properties than previously thought. While these findings oppose the results of control experiments and previous studies, they are important in forwarding the discussion of the role that organic aerosol, in particular SSA, play in cloud droplet activation.

In addition, the results of this work suggest that differences in organic composition between the SML and bulk water samples are insignificant on the hygroscopic properties. Comparisons of hygroscopicity measurements from the SML and bulk water samples do not show a significant trend, which could imply that the organic constituents in the seawater are similar between the two sample types. Furthermore, as biological activity in the ocean changes seasonally, we predicted that the organic composition of sea spray particles to change seasonally as well. There was no trend identified between the hygroscopic measurements taken from the months sampled; however, as only three months were used in the comparison, the results remain inconclusive. Additional measurements over a longer time scale are necessary to further constrain the influence of temporal changes in oceanic organic composition in SSA and its influences on CCN activation.

5.2 Future Work

As the results of this project are inconclusive, the research presented herein is still a work in progress. The mechanism contributing to the significant reduction in the hygroscopicity of the dialyzed samples has yet to be constrained; thus, future work should aim to resolve the inconsistencies. In the discussion of the results, possible sources of systematic error are presented, as well as several other factors which may contribute to our observations. These areas should form the focus of future research, as discussed below.

Before exploring other possible explanations, the first approach to resolving the unexpected results should focus on measurements of the volume fractions of components in the atomized particles. Three different methods were previously attempted to verify the composition of the particles from the seawater solutions (Appendix C). Each of the methods has yet to provide conclusive results; further refinement of the mass spectrometry, filter, and fluorescence microscopy methods can be carried out for validation. The previous attempts did not focus on specific characterization of the particle sizes relevant to the hygroscopicity measurements. As such, designing further experiments of this nature would be best approached with a particular focus on analyzing particles in the 50-100 nm size range. While each method could be modified to account for particles of this size, the filter technique may be the easiest to implement of the attempted methods by simply size selecting the particles prior to loading them on a filter. Composition measurements using the other attempted techniques are still possible, however, refining the methods may pose additional challenges in chemical analysis and size selection for the ACSM and fluorescence microscopy, respectively. Specifically, the ACSM method

requires further diagnostic testing to determine the cause of deviations in measured and delivered concentrations, and a method for loading 50 – 100 nm particles onto hydrophobic slides is necessary in order to perform fluorescence microscopy on particles of this size range.

In addition to characterizing the methods further, subtle adjustments to the current method of processing samples could provide further insight to the mechanisms contributing to our unexpected results. The samples presented in this thesis were raw seawater samples, with no additional processing except for dialysis. As such, filtration of the seawater samples using a 0.45 μm filter (or smaller) will allow for a better understanding of the sample composition with respect to size and solubility. Filtering the seawater prior to processing and analysis would remove particulate organic material from the samples, leaving behind only the dissolved organic components. Analyses conducted on filtered samples should be given future consideration as particulate constituents present in the atomized solutions could break apart and produce in externally mixed particles, resulting in particle compositions that deviate from expected (Section 4.5.2).

As there are a variety of dialysis membranes commercially available with different pore sizes, comparisons can be made between dialyzed samples with different MWCO membranes. Since the properties of organic components typically depend on size, these experiments could provide further constraint on the size of the compounds that remain in the sample and allow for further inference on the organic properties. For example, using a membrane with a higher MWCO may permit for removal of DOM in seawater, allowing for the hygroscopic properties of the particulate and less soluble organic material to be

characterized. Likewise, using a larger MWCO may increase the desalting efficiency of the dialysis process. Characterization of the samples over a wider range of sea salt concentrations could also be useful at providing insight. As such, by varying the length of time that the samples are dialyzed, the change of hygroscopicity in a single sample could be characterized as a function of inorganic removal and to better understand when and how the deviation from expectations occurs.

In the theoretical predictions used in this thesis, solubility and surface tension effects were not taken into account. Instead, the surface tension of water was used in calculations (Section 1.3), and the κ-Köhler curves were modeled without consideration of solubility or phase separation behavior. Since surface active compounds are able to lower the surface tension on an activating cloud droplet and reduce the particle activation diameter, we do not expect that surface tension effects account for the differences between measured and predicted κ_{inf} in the experiments as this effect would yield higher measured hygroscopicities. On the other hand, solubility and phase separation may have the opposite effect, as previously discussed in Section 4.5.3. Additional experiments conducted on control solutions could further the characterization of the results. In the control experiments presented in this work, mannitol, which is highly soluble, was used as a model organic compound. Further tests using additional organic compounds with different properties (i.e. solubility, surface tension, etc.) as model organic compounds may be useful for comparisons with theoretical predictions because these properties can also influence particle hygroscopicity, and the seawater samples are expected to contain organics with a variety of properties. Specifically, control experiments could be performed with organic compounds that are less soluble and compounds that are known to phase

separate in mixed component particles, such as 1,6-hexanediol. Furthermore, the control solutions could be prepared with a wider range of organic/inorganic mass ratios, especially at ratios that mimic the observed volume fractions of the seawater solutions after dialysis (Section 4.3.3).

In addition to further control experiments, more work should be done with seawater from different locations as well. First of all, it is important to note that the differences observed between the SML and bulk water samples were found to be insignificant; both sample types show the unexpected hygroscopic behavior during measurements. Therefore, the experiments suggested for future work could be performed on bulk water, which is easier to collect in larger volumes in shorter amounts of time. Likewise, all of the experimental results for seawater presented in this work are for samples taken from the Northwest Arm in Halifax, Nova Scotia. The Northwest Arm, which is an estuary, is likely not representative of open ocean water. Similarly, samples from the Northwest Arm may have contamination due to anthropogenic influence from boat traffic and boat yards. As a result, further experiments should be carried out on water from different locations, ideally from areas away from significant anthropogenic pollution sources and further offshore. Furthermore, to gain additional insight on seasonal variations in seawater chemistry and its influence on hygroscopic properties, samples could be collected over a larger variety of seasons. Particularly, hygroscopicity measurements of particles generated from seawater before, after, and during periods of biological activity would be of interest when combined with oceanographic data of the ocean biology.

Additional experiments could be conducted using different methods of particle generation as well. As SSA from the ocean form primarily due to bubble bursting processes, the laboratory methods used for previous experiments could be adapted to measure the hygroscopicity of particles generated from a bubbler. The use of a bubbler to generate particles will result in particles that are enriched in organic composition relative to seawater (Section 2.3). The particles with higher enrichments of organics will allow for the characterization of a greater range of organic volume fractions which are also produced from a more natural source. While these measurements could be useful for resolving the discrepancies between the measured and expected hygroscopicities, using a bubbler has its disadvantages as well. First, the volume fractions of the organic composition in the particles are expected change as a function of size when produced from a bubbler. As such, a method to determine the composition of the bubbled particles between 50 – 100 nm will require further development before the hygroscopicity data can be analyzed according to theory (Appendix C). Also, as the mass of organic matter in the seawater samples is low, it is possible that bubbling the seawater will deplete the organics from solution on timescales that are too short to conduct hygroscopicity experiments. Therefore, methods for measuring volume fraction and organic removal during bubbling need to be further characterized to implement measurements of bubbled particles to further this work.

5.3 Atmospheric Implications

As previously discussed, it is possible that the results are a systematic artefact from sample processing or instrumental analysis. For instance, the composition of the atomized particles may be different from the calculations using seawater chemistry, as discussed in

Section 3.5. In the case of systematic error, we cannot speculate on the atmospheric implications of the results presented herein. Instead, this work may provide further evidence of the suggested effects of surface active organic material on the composition of atomized particles (section 4.5.2). In addition, the current work could serve to verify that previous studies using the same assumption with an atomizer are not valid. While these results would be significant in the approach to future laboratory studies using atomization, further characterization of the volume fraction of organic components in the atomized aerosol is necessary to draw such conclusions.

In the atmosphere, the results of the present work suggest that organic composition reduces the hygroscopicity in SSA more significantly than evidenced by previous studies. If the results are due to a mechanism other than systematic error, the inclusion of a small percentage of organic constituents ($< 2\%$) in sea salt particles may decrease the concentration of CCN in the marine boundary layer, thereby lessening the reflectivity and lifetime of clouds over the ocean. Capturing the reduction of these effects in model simulations could enhance the representation of aerosol indirect effects and improve the credibility of future climate projections.

As SSA number concentrations are most abundant at CCN relevant sizes with significant organic enrichment, these results may hold a considerable influence on aerosol-cloud interactions in the atmosphere. The reduction in CCN concentrations in the marine boundary layer could have important ramifications for the cooling effect associated with the indirect effect of aerosols, suggesting that the cooling potential is less significant than previously identified. The magnitude of this effect is likely to be most prominent in

locations where anthropogenic influence is negligible, such as remote regions over the

open ocean and the summertime Arctic atmosphere. Since these regions comprise a large

fraction of Earth's surface and may be most sensitive to small changes in CCN

concentrations, a better understanding of the mechanism contributing to reduced

hygroscopicity resulting from organic compositions could further constrain the uncertainty

of the indirect effect associated with SSA, an important source of natural aerosol

emissions to the atmosphere.

Appendix A

A.1 Summary of Chemical Analyses of Seawater

Table A.1   Summary of the chemical analyses of seawater samples.

Month	Sample	Salinity	TOC (µmol/L)	OM (g/L)	ε_{inorg}	ε_{org}
September	SML	29.89	266.6	0.0045	99.99%	0.01%
	Dialyzed SML	0.52	260.2	0.0044	98.90%	1.10%
	Bulk	28.6	116.7	0.0020	99.99%	0.01%
	Dialyzed Bulk	0.55	308	0.0052	98.80%	1.20%
November	SML	33.54	128.55	0.0022	99.99%	0.01%
	Dialyzed SML	0.62	103.28	0.0017	99.60%	0.40%
	Bulk	36.03	101.66	0.0017	99.99%	0.01%
	Dialyzed Bulk	0.53	196	0.0033	99.20%	0.08%
January	SML*	34.93	6171.3	0.1038	99.70%	0.30%
	Dialyzed SML	0.40	335.9	0.0056	98.60%	1.40%
	Bulk	34.74	122.3	0.0021	99.99%	0.01%
	Dialyzed Bulk	0.29	347.4	0.0058	97.99%	2.01%

*Organic contamination suspected in sample.

Appendix B

B.1 Dialysis Method Development

Table B.1   Summary of the tests performed to develop a dialysis method for processing
seawater samples.

Test #	Description	Solution	Initial Conc. (g L^{-1})	Final Conc. (g L^{-1})	Runtime (hours)	Results
1	Initial test, recycling dialysate	NaCl	35	0.015	47	Inorganic concentration significantly reduced
2	Initial test, recycling dialysate	Filtered SW	30-35	0.009	51	Inorganic concentration significantly reduced
3	Dialysate overflow, higher circulation rate	NaCl	35	0.03	27	Dialysate overflow improves time efficiency of inorganic removal
4	Dialysis using stir plate	Filtered SW	30-35	0.294	70	The stir plate is less effective than dialysate overflow
5	Dialysate overflow, setup in refrigerator*	Filtered SW	30-35	0.053	160	Longer time required, effective removal of inorganics
6	Low Mw organic retention	L-Tryptophan	0.399	0.279	48	~70% retention of L-Tryptophan
7	High Mw organic retention	Erythrosin B	0.393	0.093	48	Dye bound to membrane, inconclusive

*The method used for processing the collected seawater samples.

The first step in the method development process focused on characterizing the removal

efficiency of the dissolved salts in seawater. These first-order tests were designed to be as

simple as possible and were only intended to examine the feasibility of using dialysis to

desalt a solution as highly concentrated as seawater. Test #1 was performed with a NaCl

solution, prepared to have a concentration similar to natural seawater (35 g NaCl L^{-1}), and

test #2 used filtered seawater collected from taps operated and maintained by the

Department of Oceanography at Dalhousie University. The trials were run at room

temperature with a small peristaltic pump (Adafruit 1150) to cycle the dialysate at a rate of

100 mL min^{-1} through a 1 L graduated cylinder containing the dialyzing sample. The

graduated cylinder was placed inside of a larger reservoir, allowing the overflowing of deionized water from the beaker to be collected and recycled back through the system. The deionized water was replaced periodically to ensure that equilibrium was not reached between the sample and the dialysate such that molecular diffusion continued to occur. Using ion chromatography (IC) to quantify chloride ion concentrations in the test solutions, the salinity was determined for each sample before and after dialysis. For seawater, the salinity (ppt) of a sample can be calculated by multiplying the chloride ion concentration (mg L^{-1}) by 0.0018066 (Johnson et al., 2007).

The analytical results of tests 1 & 2 demonstrate that the salinity of both the NaCl solution and the filtered seawater were significantly reduced after two days of dialysis. The initial salt concentration of 35 g L^{-1} was reduced to 0.015 and 0.009 g L^{-1} for the NaCl solution and filtered seawater, respectively. The variation between the NaCl solution and the seawater is likely due to the timing and frequency of dialysate changes. The results provide proof of concept that dialysis could be used to significantly reduce the inorganic salt concentration from highly concentrated seawater samples.

A series of other tests were designed to refine the dialysis technique and cater it to the specific needs of the research in this thesis. Specifically, further tests were performed to characterize the amount of salt removed, the length of time required, the best mechanism for cycling water through the system, and the retention of organic compounds with molecular weights above and below 500 g mol^{-1}.

The approach for dialysis test #3 was similar to the initial tests, but small changes were made to the dialysate circulation system. In the case of the first two tests, the dialyzing potential of the dialysate was reduced over time because the salts that diffuse from the sample increase in the dialysate reservoir until the reservoir was changed. As such, for the third test, the dialysate was not recycled. Instead, the graduated cylinder was placed in a sink, and deionized water was pumped into the graduated cylinder from a separate reservoir, allowing all overflow from the graduated cylinder to drain down the sink. This mechanism of cycling water through the graduated cylinder permits replacement of the dialysate while preventing the dialysis membrane from drying out. The reservoir was refilled with deionized water each time it was emptied by the pump. In addition, a larger pump, capable of pumping 1 L min^{-1}, was used such that a larger volume of dialysate could be cycled through the system. The test was performed on a NaCl solution (35 g L^{-1}).

The results from the third test show that the sample had a conductivity lower than tap water after about a day of dialyzing. Test #3 required approximately 50% of the time of the tests 1 & 2 and yielded a similar reduction in salt from the sample. Since a larger pump was used for this experiment, a greater volume of dialysate was cycled through the system. Also, as the overflow from the graduated cylinder was allowed to drain down the sink, the salt concentration in the dialysate remained lower. Thus, the dialysate was able to maintain a higher concentration gradient, and dialysis occurred more quickly.

A fourth test aimed to further reduce the dialysis time and increase desalting efficiency. For test #4, dialysis was conducted on a NaCl solution (35 g L^{-1}) in a 500 mL beaker while using a stir plate. The stir place can introduce turbulence into the system, which may

increase the diffusion of dissolved inorganic ions from the sample and improve the speed and capacity of desalting. The dialysate was changed manually at periodic intervals, and a small volume of the dialysate and sample were taken during each dialysate change to examine concentration gradients and the progress of dialysis.

Using the stir plate did not prove to be advantageous over the pump circulation system employed in test #3. First, there were issues with the stir bar interfering with and potentially damaging the dialysis membrane. Due to the interference, the use of the stir plate had be cut short to avoid compromising the integrity of the membrane. Analyses of the salt concentration in the sample while using the stir plate indicate that the salt concentration reduced more slowly than test #3. Such a result suggests a greater dialysate volume is more effective for desalting than using a stir rod. In addition, when the water is cycled using a pump, the flow of water past the tubing creates a small amount of turbulence. Therefore, using a peristaltic pump with a flowrate of 1 L min^{-1} to cycle deionized water through a graduated cylinder was found to be the most efficient dialysis method, especially when the dialysate is not recycled.

The measured concentration gradients throughout test #4 also provide insight into the time required for equilibrium between the sample and the dialysate. After as long as 3 hours, the sample and the dialysate were not in equilibrium even while stirring and using a smaller dialysate volume. The observation that a long length of time is required to reach equilibrium indicates that the timing of the dialysate circulation pump can be slowed such that manual refilling of the dialysate is not required as frequently. As a result, the dialysis system can persist for longer periods of time without maintenance.

Since seawater contains DOM that is subject to temperature and photodegradation, the dialysis process should take place at 4˚C and in the dark to limit the loss of the sensitive organic compounds (Chen and Wangersky, 1996). Colder temperatures also decrease the molecular diffusion of dissolved ions in a solution, which would impact the time efficiency of dialysis. Test #5 was designed to quantify the dialyzing potential of a seawater solution at 4˚C with respect to time. The test used a modified setup of the peristaltic pumping design from test #3 that could be employed in a refrigerator: the dialysis sample was placed in a 1 L beaker and deionized water was pumped through the beaker from a reservoir. Instead of draining down the sink, dialysate overflow from the beaker was collected inside of a catch basin. The catch basin was emptied each time the dialysate reservoir was refilled to avoid flooding the refrigerator. The test was conducted on filtered seawater and lasted for 1 week. A small volume of the seawater sample was collected during the course of dialysis to evaluate the change in salinity as a function of time.

The results from test #5 show that the concentration of inorganic salts in the seawater are reduced to the concentration of tap water after one week of dialysis. Due to the high concentration gradient present at the start, the majority of the inorganics were lost during the first two days of the test. After the sharp initial reduction, the salinity continued to decrease, but at a much slower rate. The level of desalting that occurring in the final two days of dialysis was minimal, suggesting that the length of time for dialysis could be reduced to 5 days. In addition, this test used real seawater, which confirms that the inorganics can be substantially decreased in samples collected from the ocean while

minimizing the degradation of temperature and photosensitive organics. As the results were successful, all subsequent seawater samples discussed in this thesis were dialyzed using the refrigerator setup employed in test #5.

Once the mechanism for dialysis on seawater used in this thesis was developed, additional tests were carried out to characterize the retention of organic compounds during dialysis. The MWCO of the selected dialysis membrane is 100 - 500 Da, meaning that the membrane will allow components with molecular weights below 100 - 500 g mol^{-1} to diffuse through. As the organic composition of the seawater is expected to vary greatly, organics of high and low molecular weights are likely to be present in the samples. While this size range is sufficient for the removal of dissolved inorganic salts, it may result in the removal of some low molecular weight organic compounds as well. Therefore, to further characterize the method, it was necessary to quantify the retention of the organic components in the dialyzed sample.

The procedure to test for retention was to perform dialysis on a sample that was spiked with a known concentration of an organic compound and then quantify the concentration that remains after dialysis. As certain groups of organic compounds possess absorbance properties in the UV/visible spectrum, their concentrations can be quantified using a spectrophotometer. As such, the selected compounds must exhibit absorption. Furthermore, I was interested in evaluating the retention of compounds that have molecular weights above and below the MWCO of the membrane. L-Tryptophan was selected as a low molecular weight compound (Mw = 204.23 g mol^{-1}), and Erythrosin-B (Mw= 879 g mol^{-1}) was selected as a high molecular weight compound. Due to their

aromatic structure, L-Tryptophan and Erythrosin-B both exhibit strong absorbance of UV/visible light. Stock solutions of Erythrosin-B and L-Tryptophan were prepared and individually dialyzed in a refrigerator for 2 days. Several dilutions of the stock solutions were analyzed using a UV-Vis-NIR spectrophotometer (Cary 5000, Varian Inc.) to prepare a calibration curve such that the quantification of the samples after dialysis was possible.

After two days of dialyzing, ~70% of L-Tryptophan was retained in the solution. The result is not surprising, considering that the molecular mass of L-Tryptophan falls within the range of the dialysis membrane's MWCO. The loss of ~30 % L-Tryptophan during dialysis provides evidence that a fraction amount of the low molecular weight organic compounds in seawater will be lost during the processing of real seawater samples.

For Erythrosin-B, the retention test results are inconclusive. The quantitative results indicate that only 20% of Erythrosin-B was present in solution after 2 days of dialysis; however, Erythrosin-B is a very strong dye, which is often used as food coloring agent (Chequer et al., 2012). Upon completion of the dialysis test on Erythrosin-B, the membrane was stained red, which suggests that complete recovery of the Erythrosin-B from the membrane is not possible. Incomplete recovery impedes the reliability of a quantitative evaluation of retention. Nevertheless, as dialysis is a proven method to separate dissolved constituents based on mass (Ungaro et al, 2012) and the molecular weight of most organic compounds in the ocean are much greater than the MWCO of the selected membrane (Moore et al., 2008; Cunliffe et al., 2013), the assumption that large

molecular weight organic compounds in seawater will be retained during dialysis is

reasonable.

APPENDIX C

C.1 Tests for Atomization Assumptions

C.1.1 Aerosol Mass Spectrometry

The mass spectrometry method was considered as a means of obtaining direct measurements of the atomized particle compositions. A mass spectrometer is an instrument capable of analyzing the chemical components in a sample. In this case, an Aerosol Chemical Speciation Monitor (ACSM, Aerodyne) was used to measure the mass concentration ($\mu g \ m^{-3}$) of different chemical species in particles. The ACSM, which is modeled after the more elaborate Aerosol Mass Spectrometer, provides a lower cost, low maintenance alternative to characterize chemical composition in submicron aerosol. In the instrument, the particle flow is focused into a narrow stream, vaporized in an oven, and then chemically speciated using a quadrupole mass spectrometer. Mass concentrations can be characterized for particles 40 nm – 1 μm with a 15 – 30 minute time resolution (Ng et al., 2011).

Prior to use, an external calibration of the ACSM was performed with pure ammonium nitrate particles. The particles were generated from an atomizer, size selected using an electrostatic classifier, and counted using a Condensation Particle Counter. Since the composition is known and the number concentrations of the particles delivered to the ACSM are measured, mass concentrations can be calculated. The particle stream from the atomizer was diluted with a controlled source of filter compressed air, and the volume of

dilution flow was changed between measurements to deliver various mass concentrations to the instrument. From these measurements, the ACSM generates a calibration curve that relates the detector measurements to the true/delivered mass concentrations.

An additional calibration procedure for the ACSM was attempted for mixed organic/inorganic particles. For this procedure, mannitol and ammonium nitrate were used as model organic and inorganic components in the particles, respectively. It is important to note that ammonium nitrate is used in place of NaCl due to the high vaporization temperature of NaCl (1465˚C). The operating temperature of the oven in the ACSM is 600˚C; hence, NaCl does not undergo ionization and is undetectable in the ACSM. Three solutions were prepared for calibrations; pure mannitol, pure ammonium nitrate, and a 50/50% mixture of mannitol and ammonium nitrate by mass. The calibrations were performed according to the same procedure as pure ammonium nitrate particles, as previously discussed.

The results of the internally mixed aerosol calibrations with the ACSM are summarized in Figure C.1. While the concentrations of mannitol show considerable agreement, the measured ACSM concentrations of ammonium nitrate and the 50/50 mixture during these experiments are not as expected. A calibration with ammonium nitrate was performed just prior to these experiments, yet, there is significant deviation between the measured and delivered concentrations. Furthermore, the mass concentration of the mixed solution does not agree with the expectations. Considering that the mixed particles are composed of
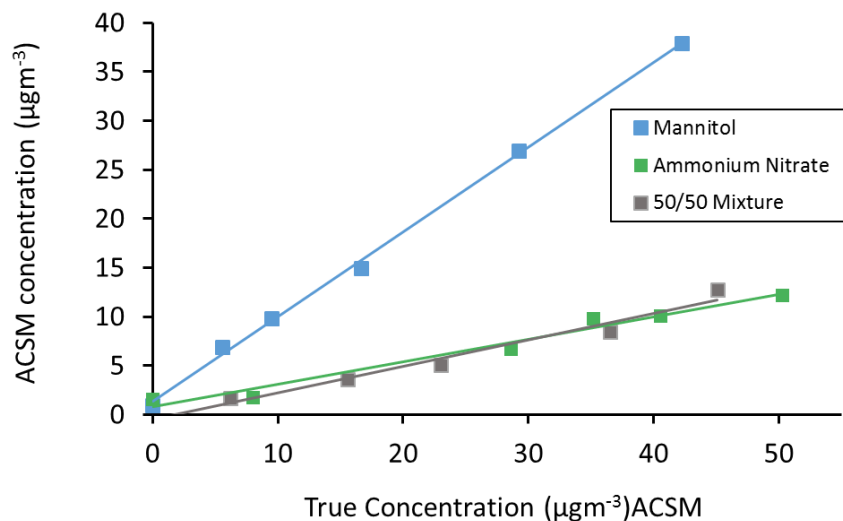
Figure C.1   Mixed component particle calibrations using an ACSM. Particles were size selected at 200 nm, and diluted with varying amounts of particle free air. Each data point represents a scan period of 15 minutes.

mannitol and ammonium nitrate, measured prior to the mixed particle experiment, the concentrations measured by the ACSM were hypothesized to be additive of the results for the model organic and inorganic compounds. Instead, the reported concentrations are much lower than the true aerosol mass delivered to the ACSM. Given these results, additional experiments were not attempted and the cause of the low concentrations remains unknown. Further characterization of the mass spectrometry method for determining the composition of particles from an atomizer represents an area of future work, possibly using the more sophisticated Aerosol Mass Spectrometer which is capable of analyzing size resolved particle compositions.

C.1.2 Filter Experiments

Techniques for aerosol filter measurements are well developed and are the most common approach for aerosol mass concentration measurements (McMurry, 2000). As such, we

considered filtration as a suitable method for measuring the volume fraction of chemical components in the atomized seawater samples. The experimental design is simple: atomized particles are collected on filters, extracted in aqueous solutions, and analyzed using analytical chemistry techniques. In order to test the method, we designed a series of experiments on control solutions prior to seawater samples. Single-component and mixed solutions were prepared using mannitol and NaCl. The atomized particles were collected using 25 mm PTFE filters (225-2726, SKC) in a filter housing designed and manufactured by AirPhoton, LLC for the Surface PARTiculate mAtter Network (SPARTAN), and the SPARTAN methods were used for filter weighing, extraction, and chemical analysis using ion chromatography (IC) (Snider et al., 2015). The Extended Aerosol Inorganic Model (http://www.aim.env.uea.ac.uk/aim/aim.php) was used to correct the measurements of filter weight for particle water uptake according to ambient relative humidity conditions (Clegg, 1998; Wexler and Clegg, 2002).

Trials were attempted where 300nm particles were size selected using a DMA and counted using a CPC to determine the particulate mass delivered to the filters. Likewise, additional tests were carried out where the atomizer spray was collected directly on the filters. Comparisons of the mass from filter weights, the delivered particle mass from CPC concentrations, and IC analyses were not equivalent, and no apparent trend was recognized in the data. For example, for pure NaCl particles, the masses of NaCl measured using IC were much lower than the masses obtained by weighing the filters. Performing these experiments under replicate conditions did not provide further insight to the mechanism causing the differences between the mass measurements, such as errors with water uptake calculations, extraction efficiency, or measurement errors, as the magnitude

of difference between each trial was inconsistent. Refinement of the filtration method for particle characterization from the atomizer experiments can be undertaken in future work. Additional experiments beyond the failed control tests were not explored in this thesis.

C.1.3 Fluorescence Microscopy

Fluorescence procedures have long been used in the biological sciences (e.g. Hobbie et al., 1977) to identify and characterize organic compounds. The technique of fluorescence microscopy can be applied to atmospheric aerosols to classify the presence and abundance of organic components, including biogenically sourced organics, in particles of mixed organic/inorganic compositions (Pan, 2014). As a result, a method of fluorescence microscopy was employed to visually detect the magnitude of the organic fraction in the particles from the atomized seawater solutions.

For the analysis, atomized particles were sprayed into an Andersen Cascade Impactor (Andersen 2000) as wet droplets to be size selected. The impactor operates at a flow rate of 28.3 L min^{-1}, and has 7 stages. Each stage in the impactor has an associated size cut which characterizes the size of the particles which are able to pass through the stage; each successive stage allows for smaller particles to be collected onto impaction plates. Siliconized glass coverslips (Hampton Research, HR3-215) were placed on the bottom stage of the impactor to collect droplets < 430 nm (Hata et al., 2012). The siliconized coverslips provide a hydrophobic surface on which the droplets are collected and can remain spherical in shape. The resulting particles were viewed on a microscope and imaged with a camera capable of representing the scale. The particles were exposed to

relative humidity between 90 – 95%, causing the particles to uptake water and coalesce.

Figure C.2 shows images of the collected particles before and after humidification.
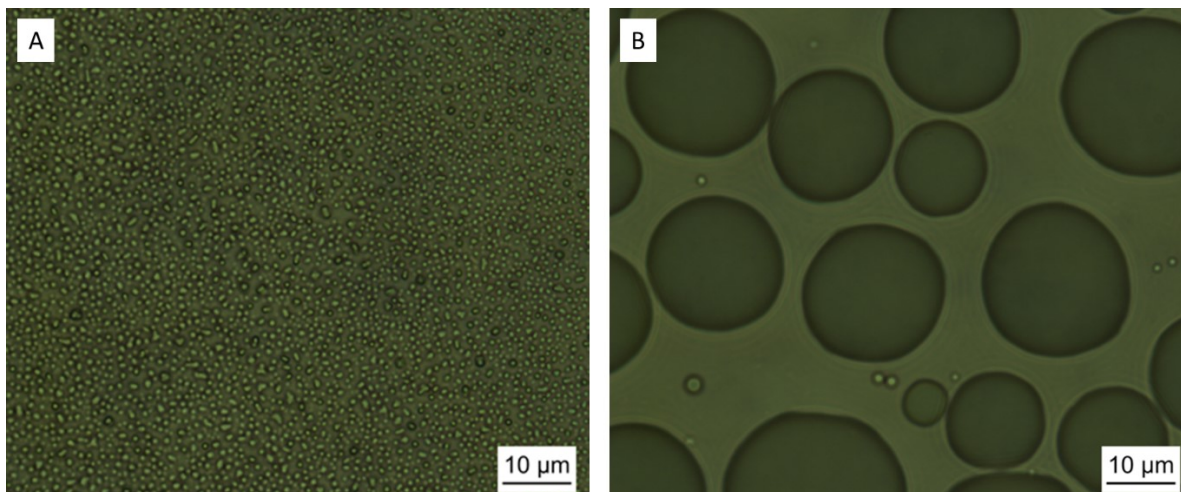

Figure C.2   An image of atomized seawater particles before and after humidification. Image A shows the collected particles before exposure to humidity, and image B illustrates water uptake and the coalescence of the particles after being humidified. Upon drying out, the resulting particles fall in the range of 10 - 20 microns, allowing them to be analyzed via fluorescence microscopy.

The fluorescence analysis was carried out by Dr. James Grayson of the Bertram Group at the University of British Columbia on an atomized bulk seawater sample before and after dialysis as well as a bubbled seawater sample. Particles generated from a bubbler were included such that a sample of enhanced organic enrichment was observed. The samples were analyzed according to the method described by You et al. (2012). The results are as expected; very little organic was found in the particles from the bulk seawater, and the bubbled particles contained a significant amount of organics (estimated 40% of particle volume). The dialyzed sample could not to be analyzed due to insufficient particle mass on the hydrophobic coverslips. Further pursuit of these analyses could be beneficial for confirming the atomizer assumption; however, the collected particles are approximately

10 times larger than the particles observed during the hygroscopicity experiments. As such, modifying the method to repeat these experiments using the DMA for particle size selection may warrant future attention.
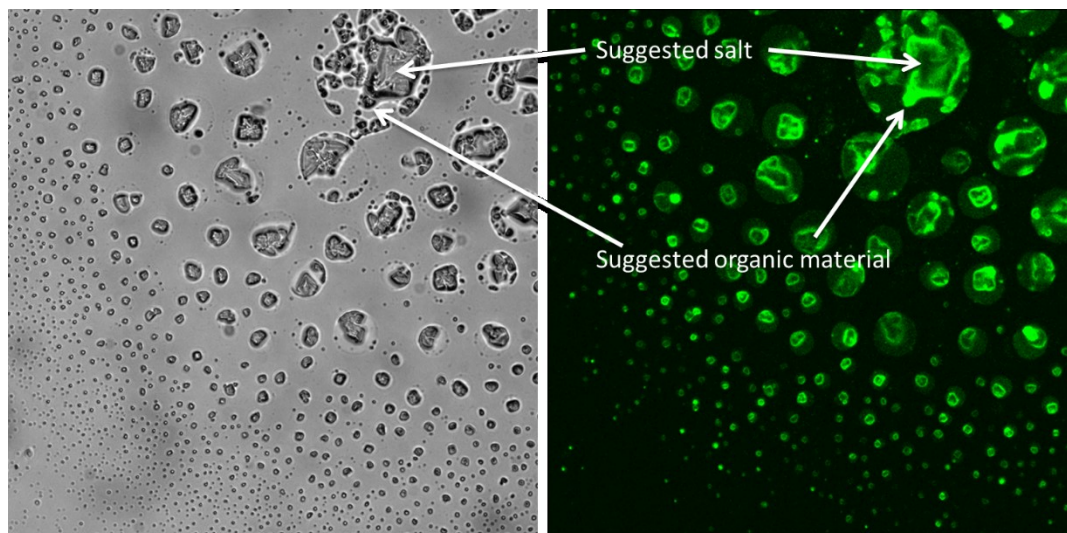

Figure C.3   Fluorescence microscope imagery for internally mixed particles containing organics and sea salt generated from a bubbler. Photo by Dr. James Grayson of University of British Columbia.

Appendix D

All figures in this thesis that were not created by the author are reproduced with copyright permission from the original publishers:

Figure 1.2   Reproduction approved by IPCC
                    (https://www.ipcc.ch/home_copyright.shtml)

Figure 2.1   Reproduced with permission from John Wiley and Sons and
                    Copyright Clearance Center, license number 4023180347883.

Figure 2.2   Reproduced with permission from Nature Publishing Group and
                    Copyright Clearance Center, license number 4023220286408.

Figure 3.4a   Reproduced with permission from Nature Publishing Group and
                    Copyright Clearance Center, license number 4023180993418.

Figure 3.4b   Reproduction permitted by TSI Inc.
                    (http://www.tsi.com/uploadedFiles/_Site_Root/Company/TSI%20C
                    opyright%20Notice.pdf)

Figure 3.5   Reproduction permitted by TSI Inc.
                    (http://www.tsi.com/uploadedFiles/_Site_Root/Company/TSI%20C
                    opyright%20Notice.pdf)

Figure 4.8   Reproduction approved under ACS AuthorChoice agreement
                    (http://pubs.acs.org/page/policy/authorchoice_termsofuse.html)

Figure 4.10   Permission granted under Creative Commons Attribution 3.0 license
                    (http://www.geoscientific-model-
                    development.net/about/licence_and_copyright.html)

Figure 2.3   Reproduction approved by American Chemical Society:

Figure 3.3   Reproduction approved by John Wiley & Sons, Inc.:

To Whom it May Concern,

My name is Matthew Boyer, and I am currently preparing my Master's thesis at Dalhousie University in Halifax, Nova Scotia, Canada.

I would like to request copyright permission to reproduce a figure in my thesis. The information is as follows:

- TITLE: Biochemistry, 4th Edition
- AUTHORS: Donald Voet, Judith G. Voet
- FIGURE INFO: Figure 6-11, Chapter 6, Page 141

Canadian graduate theses are reproduced by the Library and Archives of Canada (formerly National Library of Canada) through a non-exclusive, world-wide license to reproduce, loan, distribute, or sell theses. I am also seeking your permission for the material described above to be reproduced and distributed by the LAC(NLC). Further details about the LAC(NLC) thesis program are available on the LAC(NLC) website (www.nlc-bnc.ca).

Full Publication details and the copyright permission will be included in the thesis.

Thank you in advance for your assistance,

Matthew Boyer

Dear Mr. Boyer:

Thank you for your email.

Permission is hereby granted for the use requested subject to the usual acknowledgements (author, title of material, title of book, ourselves as publisher). You should also duplicate the copyright notice that appears in the Wiley publication; this can be found on the copyright page in the book.

Any third party material is expressly excluded from this permission. If any of the material you wish to use appears within our work with credit to another source, authorization from that source must be obtained.

This permission does not include the right to grant others permission to photocopy or otherwise reproduce this material except for accessible versions made by non-profit

organizations serving the blind, visually impaired and other persons with print disabilities (VIPs).

Sincerely,

Sheik Safdar
Permissions Coordinator II/Sr.
Copyright & Permissions
Wiley

REFERENCES

Albrecht, B. A.: Aerosols, Cloud Microphysics, and Fractional Cloudiness, Science, 245(4923), 1227–1230, 1989.

Bates, T. S., Huebert, B. J., Gras, J. L., Griffiths, F. B., and Durkee, P. A.: International Global Atmospheric Chemistry (IGAC) project's first Aerosol Characterisation Experiment (ACE 1): overview., J. Geophys. Res., 103, 16 297–16 318, 1998.

Bilde, M. and Svenningsson, B.: CCN activation of slightly soluble organics: the importance of small amounts of inorganic salt and particle phase, Tellus B, 56, 128–134, doi:10.1111/j.1600- 0889.2004.00090.x, 2004.

Blanchard, D. C.: Bursting of Bubbles at an Air Water Interface, Nature, 173, 1048–1048, 1954.

Blanchard, D. C.: The ejection of drops from the sea and their enrichment with bacteria and other materials: A review, Estuaries, 12, 127–137, 1989.

Blanchard, D. C.: The electrification of the atmosphere by particles from bubbles in the sea, Prog. Oceanogr., 1, 73–112, 1963.

Boucher, O., D. Randall, P. Artaxo, C. Bretherton, G. Feingold, P. Forster, V.-M. Kerminen, Y. Kondo, H. Liao, U. Lohmann, P. Rasch, S.K. Satheesh, S. Sherwood, B. Stevens and Zhang, X.Y.: Clouds and Aerosols. In: Climate Change 2013: The Physical Science Basis. Contribution of Working Group I to the Fifth Assessment Report of the Intergovernmental Panel on Climate Change [Stocker, T.F., D. Qin, G.-K. Plattner, M. Tignor, S.K. Allen, J. Boschung, A. Nauels, Y. Xia, V. Bex and P.M. Midgley (eds.)]. Cambridge University Press, Cambridge, United Kingdom and New York, NY, USA, 2013.

Bougiatioti, A., Nenes, A., Fountoukis, C., Kalivitis, N., Pandis, S. N., and Mihalopoulos, N.: Size-resolved CCN distributions and activation kinetics of aged continental and marine aerosol, Atmos. Chem. Phys., 11, 8791-8808, doi:10.5194/acp-11-8791-2011, 2011.

Broekhuizen, K., Pradeep Kumar, P., and Abbatt, J. P. D.: Partially soluble organics as cloud condensation nuclei: Role of trace soluble and surface active species, Geophys. Res. Lett., 31, L01107, doi:10.1029/ 2003GL018203, 2004.

Carslaw, K. S., Lee, L. A., Reddington, C. L., Pringle, K. J., Rap, A., Forster, P. M., Mann, G. W., Spracklen, D. V., Woodhouse, M. T., Regayre, L. A., and Pierce, J. R.: Large contribution of natural aerosols to uncertainty in indirect forcing, Nature, 503, 67–71, doi:10.1038/nature12674, 2013.

Cerully, K. M., Raatikainen, T., Lance, S., Tkacik, D., Tiitta, P., Petaja, T., Ehn, M., Kulmala, M., Worsnop, D. R., Laaksonen, A., Smith, J. N., and Nenes, A.: Aerosol hygroscopicity and CCN activation kinetics in a boreal forest environment during the 2007 EUCAARI campaign, Atmos. Chem. Phys. Discuss., 11, 15029–15074, doi:10.5194/acpd-11-15029-2011, 2011.

Chamaillard, K., Kleefeld, C., Jennings, S. G., Ceburnis, D., and O'Dowd, C. D.: Light scattering properties of sea-salt aerosol particles inferred from modeling studies and ground-based measurements, J. Quan. Spectrosc. Radiat. Transfer, 101, 498–511, doi:10.1016/j.jqsrt.2006.02.062, 2006.

Chen, W., and Wangersky P. J.: Rates of microbial degradation of dissolved organic carbon from phytoplankton cultures, J. Plankton Res., 18, 1521–1533, 1996.

Chequer, F. M. D., de Paula Venancio, V., Bianchi, M. D. L. P., and Antunes, L. M. G.: Genotoxic and mutagenic effects of erythrosine B, a xanthene food dye, on HepG2 cells, Food Chem. Toxicol., 50, 3447–3451, 2012.

Chingin, K., Cai, Y., Liang, J., and Chen, H.: Simultaneous preconcentration and desalting of organic solutes in aqueous solutions by bubble bursting. Anal. Chem., 88, 5033–5036, 2016.

Chylek, P., and Wong, J. G. D.: Erroneous use of the modified Köhler equation in cloud and aerosol physics applications, J. Atmos. Sci., 55, 1473–1477, doi:10.1175/1520-0469(1998)0552.0.CO;2, 1998.

Ciobanu, V. G., Marcolli, C., Krieger, U. K., Weers, U., and Peter, T.: Liquid-liquid phase separation in mixed organic/inorganic aerosol particles, J. Phys. Chem. A, 113, 10966–10978, 2009.

Clarke, A. D. and Kapustin, V.: The Shoreline Environment Aerosol Study (SEAS): a context for marine aerosol measurements influenced by a coastal environment and long-range transport, J. Atmos. Ocean. Tech., 20, 1351–1361, doi:10.1175/1520-0426(2003)0202.0.CO;2, 2003.

Clegg, S. L., Brimblecombe, P., and Wexler, A. S.: A thermodynamic model of the system H^+ - $NH4^+$ - Na^+ - $SO4^{2-}$ - $NO3^-$ - Cl^- - H2O at 298.15 K, J. Phys. Chem. A., 102, 2155-2171, 1998.

Coakley, J. A., Jr., Bernstein, R. L., and Durkee, P. A.: Effect of shipstack effluents on cloud reflectivity, Science, 237, 1020 – 1022, 1987.

Collins, D. B., Ault, A. P., Moffet, R. C., Ruppel, M. J., CuadraRodriguez, L. A., Guasco, T. L., Corrigan, C. E., Pedler, B. E., Azam, F., Aluwihare, L. I., Bertram, T. H., Roberts, G. C., Grassian, V. H., and Prather, K. A.: Impact of marine biogeochemistry on the chemical mixing state and cloud forming ability of nascent sea spray aerosol, J. Geophys. Res.-Atmos., 118, 8553– 8565, 2013.

Creamean, J. M., Lee, C., Hill, T. C., Ault, A. P., DeMott, P. J., White, A. B., Ralph, F. M., and Prather, K. A.: Chemical properties of insoluble precipitation residue particles, J. Aerosol Sci., 76, 13–27, 2014.

Cunliffe, M., Engel, A., Frka, S., Gasparovic, B., Guitart, C., Murrell, J. C., Salter, M., Stolle, C., Upstill-Goddard, R., and Wurl, O: Sea surface microlayers, A unified physicochemical and biological perspective of the air-ocean interface, Prog. Oceanogr., 109, 104–116, doi:10.1016/j.pocean.2012.08.004, 2013.

Cunliffe, M., Murrell, J.C.: The sea surface microlayer is a gelatinous biofilm, ISME Journal, 3, 1001−1003, 2009.

Cunliffe, M., Upstill-Goddard, R. C., Murrell, J. C.: Microbiology of aquatic surface microlayers, FEMS Microbiol. Rev., 35(2), 233–246, 2011.

Cunliffe, M. and Wurl, O.: Guide to best practices to study the ocean's surface, Plymouth, UK, 2014.

Dawson, K. W., Petters, M. D., Meskhidze, N., Petters, S. S., and Kreidenweis, S. M.: Hygroscopic growth and cloud droplet activation of xanthan gum as a proxy for marine hydrogels, J. Geophys. Res. Atmos.,121, doi:10.1002/2016JD025143, 2016.

Deane, G. B. and Stokes, M. D.: Scale dependence of bubble creation mechanisms in breaking waves, Nature, 418, 839–844, 2002.

de Leeuw, G., Andreas, E. L., Anguelova, M. D., Fairall, C. W., Lewis, E. R., O'Dowd, C., Schulz, M., and Schwartz, S. E.: Production flux of sea spray aerosol, Rev. Geophys., 49, RG2001, doi:10.1029/2010RG000349, 2011.

Ebling, A.M., and Landing, W.M.: Residence times of trace metals in the sea surface microlayer. 2014 Ocean Sciences Meeting, Honolulu, HI, Abstract 204, 2014.

Engelhart, G. J., Asa-Awuku, A., Nenes, A., and Pandis, S. N.: CCN activity and droplet growth kinetics of fresh and aged monoterpene secondary organic aerosol, Atmos. Chem. Phys., 8, 3937– 3949, doi:10.5194/acp-8-3937-2008, 2008.

Fitzgerald, J. W.: Marine aerosol: A review, Atmos. Environ., 25A, 533–545, 1991.

Frossard A. A., Russell L. M., Long M. S., Burrows S. M., Elliott S. M., Kieber D. J., Keene W. C., Bates T. S., Quinn P. K.:Sources and composition of submicron organic mass in marine aerosol particles, J. Geophys. Res., 119, 12977–13003, doi: 10.1002/2014JD021913, 2014.

Fuentes, E., Coe, H., Green, D., de Leeuw, G., and McFiggans, G.: Laboratory-generated primary marine aerosol via bubblebursting and atomization, Atmos. Meas. Tech., 3, 141–162, doi:10.5194/amt-3-141-2010, 2010.

Fuentes, E., Coe, H., Green, D., and McFiggans, G.: On the impacts of phytoplankton-derived organic matter on the properties of the primary marine aerosol – Part 2: Composition, hygroscopicity and cloud condensation activity, Atmos. Chem. Phys., 11, 2585– 2602, doi:10.5194/acp-11-2585-2011, 2011.

Giancola, C., De Sena, C., Fessas, D., Graziano, G. and Barone, G.: DSC studies on bovine serum albumin denaturation: Effects of ionic strength and SDS concentration. Int. J. Biol. Macromol., 20, 193-204, 1997.

Goldstein, A. H. and Galbally, I. E.: Known and unexplored organic constituents in the earth's atmosphere, Environ. Sci. Technol., 41, 1514–1521, 2007.

Grythe, H., Ström, J., Krejci, R., Quinn, P., and Stohl, A.: A review of sea-spray aerosol source functions using a large global set of sea salt aerosol concentration measurements, Atmos. Chem. Phys., 14, 1277–1297, doi:10.5194/acp-14-1277-2014, 2014.

Haririan I., Alavidjeh M. S., Khorramizadeh M. R., Ardestani M. S., Ghane Z. Z., and Namazi H.: Anionic linear-globular dendrimer-cis-platinum (II) conjugates promote cytotoxicity in vitro against different cancer cell lines, Int. J. Nanomedicine, 5, 63–75, 2010.

Harvey, G.W., and Burzell, L.A.: A simple microlayer method for small samples, Limnol. Oceanogr., 11, 156–157, 1972.

Hata, M., Linfa, B., Otani, Y. and Furuuchi, M.: Performance Evaluation of an Anderson Cascade Impactor with an Additional Stage for Nanoparticle Sampling, Aerosol Air Qual. Res., 12, 1041–1048, 2012.

Hewitt, G. W.: The charging of small particles for electrostatic precipitation, Trans. Am. Znst. Elect. Engrs., 76, 300-306, 1957.

Hobbie, J. E., Daley, R. J., and Jasper, S.: Use of nucleopore filters for counting bacteria by fluorescence microscopy, Appl. Environ. Microbiol., 33, 1225–1228, 1977.

Hodas, N., Zuend, A., Mui, W., Flagan, R. C., and Seinfeld, J. H.: Influence of particle-phase state on the hygroscopic behavior of mixed organic–inorganic aerosols, Atmos. Chem. Phys., 15, 5027-5045, doi:10.5194/acp-15-5027-2015, 2015.

IPCC: Summary for Policymakers, in Climate Change 2013: The Physical Science Basis, edited by T. F. Stocker, D. Quin, G.-K. Plattner, M. Tignor, S. K. Allen, J. Boschung, A. Nauels, Y. Xia, V. Bex, and P. M. Midgley, Cambridge University Press, Cambridge and New York., 2013.

Johnson, R. L., Holmquist, D. D., Redding, K.: Water Quality with Vernier, Vernier Soft and Technology, ISBN: 1-929075-45-6, 2007.

King, S. M., Butcher, A. C., Rosenoern, T., Coz, E., Lieke, K. I., de Leeuw, G., Nilsson, E. D., and Bilde, M.: Investigating primary marine aerosol properties: CCN activity of sea salt and mixed inorganic–organic particles, Environ. Sci. Technol., 46, 10405– 10412, doi:10.1021/es300574u, 2012.

Kleefeld, C., O'Dowd, C. D., O'Reilly, S., Jennings, S. G., Aalto, P., Becker, E., Kunz, G., and de Leeuw, G.: Relative contribution of submicron and supermicron particles to aerosol light scattering in the marine boundary layer, J. Geophys. Res., 107(D19), 8103, doi:10.1029/2000JD000262, 2002.

Köhler, H.: The nucleus in and the growth of hygroscopic droplets,Trans Farad Soc, 32, 1152–1161, 1936.

Kreidenweis, S. M., Koehler, K., DeMott, P. J., Prenni, A. J., Carrico, C., and Ervens, B.: Water activity and activation diameters from hygroscopicity data – Part I: Theory and application to inorganic salts, Atmos. Chem. Phys., 5, 1357–1370, 2005.

Khuntia, S., Majumder, S. K., and Ghosh, P.: Microbubble-aided water and wastewater purification: A review, Rev. Chem. Eng., 28, 191-221, 2012.

Leck, C. and Bigg, E. K.: Evolution of the marine aerosol– A new perspective, Geophys. Res. Lett., 32, L19803, doi:10.1029/2005GL023651, 2005.

Leck, C. and Svensson, E.: Importance of aerosol composition and mixing state for cloud droplet activation over the Arctic pack ice in summer, Atmos. Chem. Phys., 15, 2545-2568, doi:10.5194/acp-15-2545-2015, 2015.

Lewis, E. and Schwartz, S.: Sea Salt Aerosol Production: Mechanisms, Methods, Measurements and Models: A Critical Review, Vol. 152, Geophys. Monogr. Ser., Amer. Geophysical Union, Washington, DC, doi:10.1029/GM152, 2004.

Liger-Belair, G., Cilindre, C., Gougeon, R., Lucio, M., Gebefugi, I., Jeandet, P., and Schmitt-Kopplin, P.: Unraveling different chemical fingerprints between a champagne wine and its aerosols, P. Natl. Acad. Sci. USA, 106, 16545–16549, doi:10.1073/pnas.0906483106, 2009.

Lohmann, U. and Feichter, J.: Global indirect aerosol effects: a review, Atmos. Chem. Phys., 5, 715-737, doi:10.5194/acp-5-715-2005, 2005.

Low, R. D. H.: A generalized equation for the solution effect in droplet growth, J. Atmos. Sci., 26, 608–611, 1969.

Lu, Y., Fan, H., Stump, A., Ward, T. L., Rieker, T., and Brinker, C. J.: Aerosol-assisted self-assembly of mesostructured spherical nanoparticles, Nature, 398, 223, 1999.

Marcolli, C. and Krieger, U. K.: Phase changes during hygroscopic cycles of mixed organic/inorganic model systems of tropospheric aerosols, J. Phys. Chem. A, 110, 1881–1893, 2006.

McDonald, J. E.: Erroneous cloud-physics applications of Raoult's law, J. Meteorol., 10, 68–70, 1953.

McMurry, P. H.: A review of atmospheric aerosol measurements, Atmos. Environ., 34, 1959–1999, 2000.

Modini, R. L., Russell, L. M., Deane, G. B., and Stokes, M. D.: Effect of soluble surfactant on bubble persistence and bubbleproduced aerosol particles, J. Geophys. Res. Atmos., 118, 1388– 1400, doi:10.1002/jgrd.50186, 2013.

Moore, R. H., Ingall, E., Sorooshian, A., and Nenes, A.: Molar mass, surface tension and droplet growth kinetics of marine organics from measurement of CCN activity, Geophys. Res. Lett., 35, L07801, doi:10.1029/2008GL033350, 2008.

Murphy, D. M., Anderson, J. R., Quinn, P. K., McInnes, L. M., Brechtel, F. J., Kreidenweis, S. M., Middlebrook, A. M., Posfai, M., Thomson, D. S., and Buseck, P. R.: Influence of sea-salt on aerosol radiative rroperties in the southern ocean marine boundary layer, Nature, 392(6671), 62–65, 1998.

Murphy, S. M., Agrawal, H., Sorooshian, A., Padro, L. T., Gates, H., Hersey, S., Welch, W. A., Jung, H., Miller, J. W., Cocker, D. R., Nenes, A., Jonsson, H., Flagan, R. C., and Seinfeld, J. H.: Comprehensive simultaneous shipboard and airborne characterization of exhaust from a modern container ship at sea, Environ. Sci. Techol., 43, 4626–4640, 2009.

Nagata, T., Meon, B., and Kirchman, D. L.: Microbial degradation of peptidoglycan in seawater, Limnol. Oceanogr., 48, 745–754, 2003.

Niedermeier, D., Wex, H., Voigtländer, J., Stratmann, F., Brüggemann, E., Kiselev, A., Henk, H., and Heintzenberg, J.: LACIS-measurements and parameterization of sea-salt particle hygroscopic growth and activation, Atmos. Chem. Phys., 8, 579-590, doi:10.5194/acp-8-579-2008, 2008.

Ng, N. L., Herndon, S. C., Trimborn, A., Canagaratna, M. R., Croteau, P., Onasch, T. M., Sueper, D., Worsnop, D. R., Zhang, Q., Sun, Y. L., and Jayne, J. T.: An Aerosol Chemical Speciation Monitor (ACSM) for routine monitoring of atmospheric aerosol composition, Aerosol Sci. Technol., 45, 770–784, 2011.

O'Dowd, C. D. and de Leeuw, G.: Marine aerosol production: a review of the current knowledge, Phil. Trans. R. Soc. A, 365, 1753–1774, 2007.

O'Dowd, C. D., Facchini, M. C., Cavalli F., Ceburnis, D., Mircea, M., S. Decesari, Fuzzi, S., Yoon, Y. J. Putaud, J. P.: Biogenically driven organic contribution to marine aerosol, Nature, 431, 676– 680, 2004.

Orellana, M. V., Matrai, P. A., Leck, C., Rauschenberg, C. D., Lee, A. M., and Coz, E.: Marine microgels as a source of cloud condensation nuclei in the high Arctic, P. Natl. Acad. Sci., 108, 13612–13617, doi:10.1073/pnas.1102457108, 2011.

Padró, L. T., Moore, R. H., Zhang, X., Rastogi, N., Weber, R. J., and Nenes, A.: Mixing state and compositional effects on CCN activity and droplet growth kinetics of size-resolved CCN in an urban environment, Atmos. Chem. Phys., 12, 10239–10255, doi:10.5194/acp-12-10239-2012, 2012.

Pan, Y.-L.: Detection and characterization of biological and other organic-carbon aerosol particles in atmosphere using fluorescence, J. Quan. Spec. Rad. Trans., 150, 12–35, 2015.

Petters, M. D., and Kreidenweis, S. M.: A single parameter representation of hygroscopic growth and cloud condensation nucleus activity, Atmos. Chem. Phys., 7, 1961-1971, doi:10.5194/acp-7-1961-2007, 2007.

Petters, M. D., Kreidenweis, S. M., Snider, J. R., Koehler, K. A., Wang, Q., Prenni, A. J., and Demott, P. J.: Cloud droplet activation of polymerized organic aerosol, Tellus B, 58, 196–205, doi:10.1111/j.1600-0889.2006.00181.x, 2006.

Petters M. D., Kreidenweis S. M., Ziemann P. J.: Prediction of cloud condensation nuclei activity for organic compounds using functional group contribution methods, Geosci. Model Dev., 9, 111–124, 2016.

Petters, S. S., and Petters, M. D.: Surfactant effect on cloud condensation nuclei for two-component internally mixed aerosols, J. Geophys. Res. Atmos., 121, 1878–1895, doi:10.1002/2015JD024090, 2016.

Pilson, M.E.Q.: An introduction to the chemistry of the sea, 2nd ed., Cambridge University Press, New York, 2013.

Pradeep Kumar, P., Broekhuizen, K., and Abbatt, J. P. D.: Organic acids as cloud condensation nuclei: Laboratory studies of highly soluble and insoluble species, Atmos. Chem. Phys., 3, 509–520, 2003.

Prather, K. A., Bertram, T. H., Grassian, V. H., Deane, G. B., Stokes, M. D., DeMott, P. J., Aluwihare, L. I., Palenik, B. P., Azam, F., and Seinfeld, J. H.: Bringing the ocean into the laboratory to probe the chemical complexity of sea spray aerosol, P. Natl. Acad. Sci., 110, 7550–7555, 2013.

Pratt, K. A., and Prather, K. A.: Aircraft measurements of vertical profiles of aerosol mixing states, J. Geophys. Res., 115, D11305, 2010.

Prisle, N. L., Raatikainen, T., Laaksonen, A., and Bilde, M.: Surfactants in cloud droplet activation: mixed organic-inorganic particles, Atmos. Chem. Phys., 10, 5663-5683, doi:10.5194/acp-10-5663-2010, 2010.

Pruppacher, H. R. and Klett, J. D.: Microphysics of clouds and precipitation, 18th ed., Kluwer Academic Publishers, Dordrecht, 1997.

Quinn, P. K., Bates, T. S., Schulz, K. S., Coffman, D. J., Frossard, A. A., Russel, L. M., Keene, W. C., and Kieber, D. J.: Contribution of sea surface carbon pool to organic matter enrichment in sea spray aerosol, Nature Geo. Sci., 7, 228–232, doi:10.1038/ngeo2092, 2014.

Quinn, P. K., Collins, D. B., Grassian, V. H., and Prather, K. A.: Chemistry and Related Properties of Freshly Emitted Sea Spray Aerosol, Chem. Rev., 115, 4383–4399, doi: 10.1021/cr500713g, 2015.

Renbaum-Wolff, L., Song, M., Marcolli, C., Zhang, Y., Liu, P. F., Grayson, J. W., Geiger, F. M., Martin, S. T., and Bertram, A. K.: Observations and implications of liquid–liquid phase separation at high relative humidities in secondary organic material produced by α-pinene ozonolysis without inorganic salts, Atmos. Chem. Phys., 16, 7969-7979, doi:10.5194/acp-16-7969-2016, 2016.

Resch F. J., Darrozes J. S., Afeti G. M.: Marine liquid aerosol production from bursting of air bubbles, J. Geophys. Res. Oceans, 91, 1019–1029, 1986.

Rose, D., Gunthe, S. S., Mikhailov, E., Frank, G. P., Dusek, U., Andreae, M. O., and Pöschl, U.: Calibration and measurement uncertainties of a continuous-flow cloud condensation nuclei counter (DMT-CCNC): CCN activation of ammonium sulfate and sodium chloride aerosol particles in theory and experiment, Atmos. Chem. Phys., 8, 1153-1179, doi:10.5194/acp-8-1153-2008, 2008.

Ruehl, C. R., Chuang, P. Y., and Nenes, A.: How quickly do cloud droplets form on atmospheric particles?, Atmos. Chem. Phys., 8, 1043-1055, doi:10.5194/acp-8-1043-2008, 2008.

Russell, L. M., Hawkins, L. N., Frossard, A. A., Quinn, P. K., and Bates, T. S.: Carbohydrate-like composition submicron atmospheric particles and their production from ocean bubble bursting, P. Natl. Acad. Sci. USA, 107(15), 6652–6657, doi:10.1073/pnas.0908905107, 2010.

Schill, S. R., Collins, D. B., Lee, C., Morris, H. S., Novak, G. A., Prather, K. A., Quinn, P. K., Sultana, C. M., Tivanski, A. V., Zimmermann, K., Cappa, C. D., and Bertram, T. H.: The impact of aerosol particle mixing state on the hygroscopicity of sea spray aerosol, ACS Cent. Sci, doi: 10.1021/acscentsci.5b00174, 2015.

Schmitt-Kopplin, P., Liger-Belair, G., Koch, B. P., Flerus, R., Kattner, G., Harir, M., Kanawati, B., Lucio, M., Tziotis, D., Hertkorn, N., and Gebefugi, I.: Dissolved organic matter in sea ¨ spray: a transfer study from marine surface water to aerosols, Biogeosciences, 9, 1571–1582, doi:10.5194/bg-9-1571-2012, 2012.

Seinfeld, J. H. and Pandis, S. N.: Atmospheric Chemistry and Physics: From Air Pollution to Climate Change, 2nd ed., Wiley, Hoboken, NJ, USA, p. 444, 2006.

Sellegri, K., O'Dowd, C. D., Yoon, Y., Jennings, S., and de Leeuw, G.: Surfactants and submicron sea spray generation, J. Geophys. Res., 111, D22215, doi:10.1029/2005JD006658, 2006.

Shantz, N. C., Chang, R. Y.-W., Slowik, J. G., Vlasenko, A., Abbatt, J. P. D., and Leaitch, W. R.: Slower CCN growth kinetics of anthropogenic aerosol compared to biogenic aerosol observed at a rural site, Atmos. Chem. Phys., 10, 299-312, doi:10.5194/acp-10-299-2010, 2010.

Snider, G., Weagle, C. L., Martin, R. V., van Donkelaar, A., Conrad, K., Cunningham, D., Gordon, C., Zwicker, M., Akoshile, C., Artaxo, P., Anh, N. X., Brook, J., Dong, J., Garland, R. M., Greenwald, R., Griffith, D., He, K., Holben, B. N., Kahn, R., Koren, I., Lagrosas, N., Lestari, P., Ma, Z., Vanderlei Martins, J., Quel, E. J., Rudich, Y., Salam, A., Tripathi, S. N., Yu, C., Zhang, Q., Zhang, Y., Brauer, M., Cohen, A., Gibson, M. D., and Liu, Y.: SPARTAN: a global network to evaluate and enhance satellite-based estimates of ground-level particulate matter for global health applications, Atmos. Meas. Tech., 8, 505–521, doi:10.5194/amt-8-505-2015, 2015.

Tanaka, F., and Edwards, S. F.: Viscoelastic properties of physically crosslinked networks: Transient network theory, Macromolecules, *25*, 1516–1523, doi:10.1021/ma00031a024, 1992.

Textor, C., Schulz, M., Guibert, S., Kinne, S., Balkanski, Y., Bauer, S., Berntsen, T., Berglen, T., Boucher, O., Chin, M., Dentener, F., Diehl, T., Feichter, J., Fillmore, D., Ginoux, P., Gong, S., Grini, A., Hendricks, J., Horowitz, L., Huang, P., Isaksen, I. S. A., Iversen, T., Kloster, S., Koch, D., Kirkevåg, A., Kristjansson, J. E., Krol, M., Lauer, A., Lamarque, J. F., Liu, X., Montanaro, V., Myhre, G., Penner, J. E., Pitari, G., Reddy, M. S., Seland, Ø., Stier, P., Takemura, T., and Tie, X.: The effect of harmonized emissions on aerosol properties in global models – an AeroCom experiment, Atmos. Chem. Phys., 7, 4489–4501, doi:10.5194/acp-7-4489-2007, 2007.

Tsigaridis, K., Koch, D., and Menon, S.: Uncertainties and importance of sea spray composition on aerosol direct and indirect effects, J. Geophys. Res., 118, 220–235, doi:10.1029/2012JD018165, 2013.

Turpin, B. J. and Lim, H. J.: Species contributions to PM2.5 mass concentrations: Revisiting common assumptions for estimating organic mass, Aerosol Sci. Tech., 35, 602–610, 2001.

Twomey, S.: The influence of pollution on the shortwave albedo of clouds, J. Atmos. Sci., 34, 1149–1152, 1977.

Ungaro F., De Stefano D., Giovino C., Masuccio A., Miro A., Sorrentino R.: PEI-Engineered respirable particles delivering a decoy oligonucleotide to NF-κB: inhibiting MUC2 expression in LPS-stimulated airway epithelial cells, PLoS ONE, 7, doi:10.1371/journal.pone.0046457, 2012.

Verdugo, P., Alldredge, A. L., Azam, F., Kirchman, D. L., Passow, U., and Santschi, P. H.: The oceanic gel phase: a bridge in the DOM-POM continuum, Marine Chemistry, 92, 67–85, 2004.

Voet, D., and Voet, J. G.: Biochemistry, John Wiley & Sons, Inc., Hoboken, NJ, 2011.

Westervelt, D. M., Moore, R. H., Nenes, A., and Adams, P. J.: Effect of primary organic sea spray emissions on cloud condensation nuclei concentrations, Atmos. Chem. Phys., 12, 89–101, doi:10.5194/acp-12-89-2012, 2012.

Wex, H., Fuentes, E., Tsagkogeorgas, G., Voigtlander, J., Clauss, T., Kiselev, A., Green, D. H., Coe, H., McFiggans, G., and Stratmann, F.: The influence of algal exudate on the hygroscopicity of sea spray particles, Adv. Meteorol., 356131, doi:10.1155/2010/365131, 2010.

Wexler, A. S., and Clegg, S. L.: Atmospheric aerosol models for systems including the ions H^+, $NH4^+$, Na^+, $SO4^{2-}$, $NO3^-$, Cl^-, Br^- and H2O, J. Geophys. Res., 107, 2002.

Wu, J.: Bubbles in the near-surface ocean: A general description, J. Geophys. Res., 93, 587–590, 1988.

Wurl, O., Wurl, E., Miller, L., Johnson, K., and Vagle, S.: Formation and global distribution of sea-surface microlayers, Biogeosciences, 8, 121–135, doi:10.5194/bg-8-121-2011, 2011.

You, Y., Renbaum-Wolff, L., Carreras-Sospedra, M., Hanna, S. J., Hiranuma, N., Kamal, S., Smith, M. L., Zhang, X., Weber, R. J., Shilling, J. E., Dabdub, D., Martin, S. T., and Bertram, A. K.: Images reveal that atmospheric particles can undergo liquid–liquid phase separations, P. Natl. Acad. Sci. USA, 109, 13188-13193, doi:10.1073/pnas.1206414109, 2012.

Zhang, Q., Worsnop, D. R., Canagaratna, M. R., and Jimenez, J. L.: Hydrocarbon-like and oxygenated organic aerosols in Pittsburgh: insights into sources and processes of organic aerosols, Atmos. Chem. Phys., 5, 3289-3311, doi:10.5194/acp-5-3289-2005, 2005.

Zhang, Z., Liu, L., Liu, C., and Cai, W.: Studies on the sea surface microlayer II. The layer of sudden change of physical and chemical properties, J. Coll. Interface Sci., 264, 148–159, 2003.

Zhao, D. F., Buchholz, A., Kortner, B., Schlag, P., Rubach, F., Fuchs, H., Kiendler-Scharr, A., Tillmann, R., Wahner, A., Watne, A. K., Hallquist, M., Flores, J. M., Rudich, Y., Kristensen, K., Hansen, A. M. K., Glasius, M., Kourtchev, I., Kalberer, M., and Mentel, T. F.: Cloud condensation nuclei activity, droplet growth kinetics, and hygroscopicity of biogenic and anthropogenic secondary organic aerosol (SOA), Atmos. Chem. Phys., 16, 1105–1121, 2016.